AD-A033 482 CIVIL ENGINEERING LAB (NAVY) PORT HUENEME CALIF F/G 13/13
EVALUATION OF TOTALLY ENCLOSED ELASTOMERIC BEARING AS A HINGE J--ETC(U)
NOV 76 G WARREN
UNCLASSIFIED CEL-TN-1461 NL

1 OF 1
AD A033482

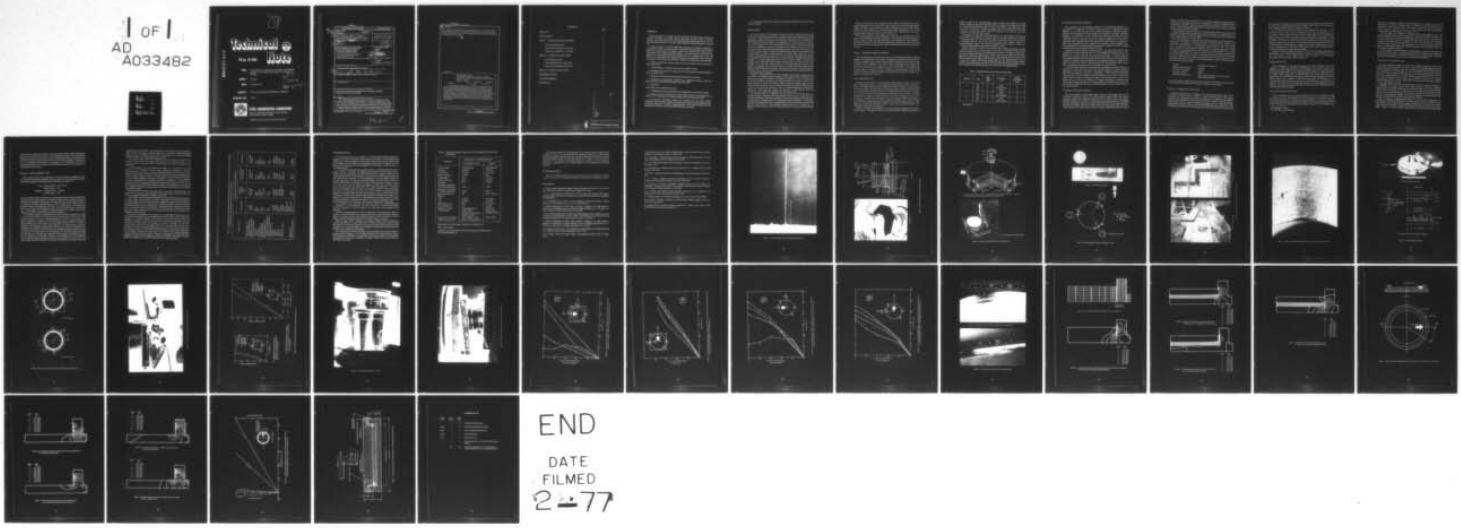

END

DATE FILMED
2-77

Technical Note

CEL

TN no. N-1461

title: EVALUATION OF TOTALLY ENCLOSED ELASTOMERIC BEARING AS A HINGE JOINT BASE OF GUYED VLF TOWER

author: G. Warren

date: November 1976

sponsor: NAVAL FACILITIES ENGINEERING COMMAND

program nos: 51-053

CIVIL ENGINEERING LABORATORY
NAVAL CONSTRUCTION BATTALION CENTER
Port Hueneme, California 93043

Unclassified

SECURITY CLASSIFICATION OF THIS PAGE (When Data Entered)

REPORT DOCUMENTATION PAGE		READ INSTRUCTIONS BEFORE COMPLETING FORM
1. REPORT NUMBER: CEL TN-1461	2. GOVT ACCESSION NO.: DN587097	3. RECIPIENT'S CATALOG NUMBER:
4. TITLE (and Subtitle): EVALUATION OF TOTALLY ENCLOSED ELASTOMERIC BEARING AS A HINGE JOINT BASE OF GUYED VLF TOWER.		5. TYPE OF REPORT & PERIOD COVERED: Final; Dec 1974 - Nov 1975
		6. PERFORMING ORG. REPORT NUMBER:
7. AUTHOR(s): G. Warren		8. CONTRACT OR GRANT NUMBER(s): 44p.
9. PERFORMING ORGANIZATION NAME AND ADDRESS: CIVIL ENGINEERING LABORATORY, Naval Construction Battalion Center, Port Hueneme, California 93043		10. PROGRAM ELEMENT, PROJECT, TASK AREA & WORK UNIT NUMBERS: O&M, N; 51-053
11. CONTROLLING OFFICE NAME AND ADDRESS: Naval Facilities Engineering Command, Alexandria, Virginia 22332		12. REPORT DATE: Nov 1976
		13. NUMBER OF PAGES: 41
14. MONITORING AGENCY NAME & ADDRESS (if different from Controlling Office)		15. SECURITY CLASS. (of this report): Unclassified
		15a. DECLASSIFICATION/DOWNGRADING SCHEDULE:

16. DISTRIBUTION STATEMENT (of this Report)

Approved for public release; distribution unlimited.

Final rept. Dec 74-Nov 75.

17. DISTRIBUTION STATEMENT (of the abstract entered in Block 20, if different from Report)

18. SUPPLEMENTARY NOTES

19. KEY WORDS (Continue on reverse side if necessary and identify by block number)

Bearing, structural rubber, finite element analysis, scratch gages, strain gages, communication towers, tower base hinge

20. ABSTRACT (Continue on reverse side if necessary and identify by block number)

The Civil Engineering Laboratory (CEL) has conducted an evaluation of a totally encased elastomeric bearing as a hinge bearing joint at the base of large guyed VLF towers. The test program included laboratory evaluation of a bearing from Andre Rubber Company, Limited, as well as a CEL-fabricated bearing; field measurements of tower base movements at Annapolis, Maryland; and finite element analysis of bearing components. Results indicate that encased elastomeric bearings similar to the Andre bearing are suitable for use as base

(continued)

DD FORM 1 JAN 73 1473 EDITION OF 1 NOV 65 IS OBSOLETE

Unclassified

SECURITY CLASSIFICATION OF THIS PAGE (When Data Entered)

391 111

20. Continued

hinges. Geometric modifications of the steel components must be made to reduce contact stresses during application of horizontal shear loads from the tower. In addition, special precaution must be taken to ensure that the elastomer is properly lubricated and is isolated from oxidation and ozone attack.

Library card

Civil Engineering Laboratory
EVALUATION OF TOTALLY ENCLOSED ELASTOMERIC BEARING AS A HINGE JOINT BASE OF GUYED VLF TOWER (final), by G. Warren
TN-1461 41 pp illus November 1976 Unclassified

1. Bearing 2. Scratch gages 1. 51-053

The Civil Engineering Laboratory (CEL) has conducted an evaluation of a totally encased elastomeric bearing as a hinge bearing joint at the base of large guyed VLF towers. The test program included laboratory evaluation of a bearing from Andre Rubber Company, Limited, as well as a CEL-fabricated bearing; field measurements of tower base movements at Annapolis, Maryland; and finite element analysis of bearing components. Results indicate that encased elastomeric bearings similar to the Andre bearing are suitable for use as base hinges. Geometric modifications of the steel components must be made to reduce contact stresses during application of horizontal shear loads from the tower. In addition, special precaution must be taken to ensure that the elastomer is properly lubricated and is isolated from oxidation and ozone attack.

CONTENTS

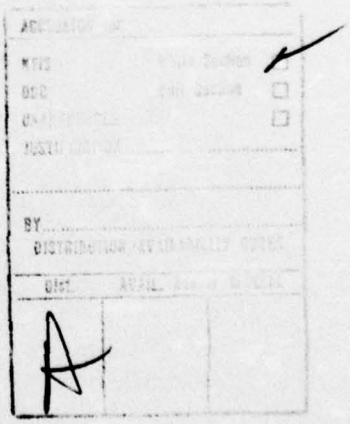

OBJECTIVE

Recent structural and material problems associated with high contact stresses and required movements in the hinge bases of large, guyed antenna towers have made it necessary to consider alternatives to steel spherical base hinges presently used [1, 2]. The most promising alternative is a totally encased elastomeric bearing developed in Germany [3].

A study was made at the Civil Engineering Laboratory, Port Hueneme, California, to determine the feasibility of employing the encased elastomeric bearing as the base hinge of guyed VLF antenna towers, an example of which is the 1,200-foot steel structure on the radio facility site at Annapolis, Maryland (Figure 1). The specific objective of the study was twofold: (1) to demonstrate that the mechanical actions (i.e., loading, rotation, twist, and shear) of the tower bases and the elastomeric bearing were compatible, and (2) to determine the longevity of the bearing. The criteria for successful use of elastomeric bearings follow:

1. Support of the antenna and guy cable structure plus resistance to effects of wind and other dynamic loads

2. Accommodation of maximum expected tower rotation and twist

3. Satisfactory performance for expected cyclic load and movement reversals during the life of the antenna tower

4. Performance with minimum maintenance during the life of the tower

5. Unaffected by environmental conditions (e.g., temperature, moisture, ozone, oil, debris, and other foreign material) during the life of the tower

6. Economical

The feasibility study consisted of four parts:

1. A bibliographical study was performed on the applications of elastomeric bearings.

2. Rotation and twist movements of the tower hinge mechanism on the large antenna at the Navy's VLF radio facility at Annapolis, Maryland, were measured and recorded.

3. An encased elastomeric bearing was purchased from the Andre Rubber Company-Limited of Ontario, Canada, and tested in the laboratory under simulated tower forces and movements. A second bearing fabricated at CEL which deviated from the manufacturer's geometric and materials specifications was also tested.

4. A finite element study was conducted on the bearing configuration subjected to axial and shear loading.

BACKGROUND

The most common use of elastomeric bearings is in bridge construction where, during the last two decades, they have performed the basic functions of transforming vertical loads from main structural members to the supporting substructures and of allowing free longitudinal translation and rotation at the supports of the superstructure [4 through 8]. The compressive stresses produced in these applications are in excess of stresses in present VLF tower bearings [1, 2]. The horizontal shear forces, which are eliminated or greatly reduced by permitting free rotation and translation in the bridge structures, are present in the antenna tower. The spherical bearing hinge employed at the base of the Navy's VLF antennas is shown in Figure 2. Analytical calculations have predicted a horizontal shear load of approximately 1/100 of the axial load with 70 minutes hinge rotation [9]. Contact stresses in the bearing were predicted to be in excess of 100 ksi. These high contact stresses are eliminated by the fluid-like behavior of an encased elastomer. Completely enclosing the elastomer in a bearing configuration such as the one shown in Figure 3a restricts the elastomer strain, allows high internal stresses in the elastomer, and overcomes the vertical instability of the elastomer. The performance of the encased elastomer is based on the property of elastomers such as rubber and neoprene to deform under load without volume change. Under high pressure the encased rubber conforms basically to hydraulic principles and behaves like a viscous fluid; thus, the concentrated contact stresses that are prevalent in a steel bearing hinge are eliminated.

Elastomeric bearing pads have been used successfully on many highway bridges since the early 1960's. The confined elastomer bearing assembly obtained from Andre Rubber and tested in this program is also shown in Figure 3b. It consisted of a circular, natural rubber pad totally enclosed by a machined, steel cylinder and piston. To prevent extrusion of the rubber between the piston and cylinder at high stresses, brass sealing rings were fitted between the piston and the rubber. The piston and cylinder were made of ASTM A36 steel. In practice the manufacturer provides a sealant of a bitumen-impregnated urethane foam between the piston plate and cylinder for protection of the elastomer from the environment. This sealant was not provided in the bearing evaluated.

The California Division of Highways has also conducted cyclic loading tests on a confined elastomer bearing with the same dimensions as the one tested in this study [6]. The California Highway bearing was subjected to cyclic horizontal shear plus rotation with a constant normal compression load of 128 kips (approximately 4,600 psi on the elastomer pad) without bearing damage. The horizontal shear load was cycled between +10 kips (0.08 times the normal load) to -10 kips, inducing bearing rotation from -1.5 degrees to +1.5 degrees about the centroidal axis of the bearing at the rate of 15 cycles per hour for 20,000 cycles.

Other tests have shown that compressive stress as high as 57,000 psi placed on the confined elastomer caused no deterioration [10]. Further, tests have shown that rubber or neoprene elastomers can be subjected to shear deformation in excess of 50% without damage. This latter capability is an important factor when considering the effect of the tower twisting about its vertical axis on the bearing. Other characteristics of the rubber elastomer will be presented in a later section of this report.

The testing performed in this program was by no means an exhaustive study. Since previous tests indicated the apparent sufficiency of the elastomer pad while subjected to cyclic and static, normal, and shear loading, the tests reported here were designed to determine the behavior of the steel-piston/cylindrical-pot assembly; e.g., the effect of the piston rubbing and bearing against the cylinder wall during horizontal shear loading plus rotation.

PHASE I – TOWER BASE HINGE MOVEMENT

The bearing hinge of the antenna tower at the Naval Station (NAVSTA), Annapolis, Maryland, was instrumented for this phase of the program to determine the behavior of the present base assembly while in service. The instrumented tower and its base hinge is shown in Figures 1 and 2, respectively. The objective of the measurements was to quantify the movement of the tower base in terms of (1) rotation of the hinge, (2) twist about the tower's vertical axis, and (3) translation normal to the vertical axis. The bearing hinge mechanism shown in Figure 2b features lubricated, precision-machined, spherical, high strength steel surfaces. The hinges, expensive to manufacture, are conducive to high contact stresses on the bearing surfaces [1, 2].

Scratch Gage Measurements

Mechanical scratch gages were incorporated to measure hinge movement. The scratch gage, a self-contained device, is used to measure and record strain and tiny movements; a 3-inch scratch gage employed for the Annapolis test is shown in Figure 4. This gage consists of two principal parts anchored to the structural subject and are capable of moving relative to each other. Relative movement between the two anchored points of the gage is scribed by the scribe arm of one portion of the gage onto a target disc on the other portion of the gage. Scratch gages are designed to sense movement in the direction parallel to the scribe arm (direction of the gage's longest dimension). The scribe arm bears slightly on the target, a 1-inch-diameter, flat brass ring. The device scribes the magnitude of the motion between two points and automatically separates sequential movements. Recordings made on the disc targets can be preserved as permanent records of data. A more detailed description of the scratch gage can be found in Reference 11.

Three sets of gages were positioned at locations around the bearing circumference as shown in Figure 5. The gages in each set were oriented in three configurations as shown in

Figure 6. Gages (A), for measuring hinge rotation movement, were oriented in a vertical direction. Gages (B) detected translational movements tangent to the hinge surface. Gage (C), mounted horizontally and in only one location, was to detect twisting movement of the hinge about the tower axis. The gages were rigidly attached by machine screws and clamps to brackets conforming to specific orientations (Figure 6). The brackets in turn were attached to the tower with epoxy cement.

The gages were in place and recorded movement for one week. During the instrumented period the tower was subjected to constant winds up to 30 mph and gusts up to 40 mph. The prevailing winds were from the south and the west during the test period. A portion of a recording scribed on one of the brass discs taken from a gage is shown in a macrophotograph in Figure 7. The maximum movement scribed on the disc is 0.035 inch. A summary of the maximum deformation is tabulated in Table 1.

Angular deformation in Table 1 was calculated from the gage deformation, assuming rotation and twist about the vertical axis of the tower. The maximum hinge rotation measured during the test period was approximately 7 minutes. The amount of twist about the tower axis measured by gage (C) was 4 minutes. There was no movement recorded in the gages (B) for measuring hinge translation. These results compare with the rotation of 70 minutes specified in the design for the bearing hinge [12]. The large discrepancy is due to the low wind velocities encountered during testing and the frictionless hinge concept employed for design analysis. It would be safe to impose the design requirements of the steel bearing plus twisting capability onto the enclosed elastomer bearing assembly.

Table 1. Maximum Movement Recorded by Scratch Gages

Gage Set[a]	Gage	Gage Length (in.)	Deformation (in.)	Angular Deformation (min)
1	(A)	6	0.020	4
	(B)	3	None detected	0
	(C)	3	0.015	3
2	(A)	6	0.025	5
	(B)	3	None detected	0
3	(A)	6	0.035	7
	(B)	3	None detected	0

[a]See Figure 5.

Requirements for Elastomer Compound

Low compression set is an important requirement of the elastomeric compound as it must support the weight of the antenna tower structure for an unlimited time with negligible set or compressive creep. Both candidate elastomeric compounds, having a hardness of 50 durometers, offer the best balance of compressive set and low temperature properties [13]. Experience has also indicated that long-term dead loads that create compressive strains in excess of 10% of the elastomer thickness will likely result in compressive creep due to cold flow and result in permanent compressive set. At compressive strain under 10%, compressive creep is less than 3% over several decades [13]; therefore, a limit of 5% is arbitrarily set on the compressive strain magnitude to ensure negligible creep. In the laboratory tests conducted during this program, the compressive strain at the design load was measured at less than 2%, well within the limit.

Neoprene and rubber exhibit a marked increase in the elastic shear modulus with reduction in temperature. Elastomers selected for bearing applications should possess a shear modulus not to exceed 200 psi [13]. At room temperature, the shear modulus for 50-durometer neoprene compounds varies between 80 and 100 psi. For natural rubber the shear modulus does not exceed 155 psi [8]. The shear stress-strain curve of both rubber and neoprene is essentially linear and independent of compressive loading up to deflections of 100% of the elastomer's thickness. Beyond this point the material stiffens sharply. Thus, a limit in design shear deformation of 25% of the thickness is considered safe.

Shear deformation characteristics are important in considering the bearing's ability to be relatively free to twist about the vertical axis of the tower (Figure 3). The shear modulus is independent of direction of deformation. This feature is important in guyed-tower hinges where the shear movement direction is unpredictable. A 25% strain for a 2-inch-thick elastomeric pad yields an allowable shear (twist) deformation of 0.5 inch. If the tower is twisted about the center of bearing, the angle of twist produced by a 0.5-inch twist deformation at a radius of 16.5 inches is 1.7 degrees (100 minutes), assuming no slip between the elastomer and steel. At 25% shear deflection, the shear stress is 20 psi for a shear modulus of 80 psi and 50 psi for a maximum modulus of 200 psi. These stresses are more than reasonable.

Comparison of Elastomeric Compounds

The long term behavior of the hinge bearing is a function of the aging resistance of the elastomeric compound. As long as the other physical properties listed above remain reasonably constant, the bearing will function for the life of the structure. The physical properties of rubber can be varied over a wide range by base elastomer selection and through variation in formulation. In addition to variations mentioned above concerning temperatures and long term loading, ozone and oxidation attacks have deteriorating effect on natural rubber properties. In contrast, there are records of neoprene applications which have shown

little, if any, deterioration after 30 years of service [7]. In addition to being impervious to oxidation and ozone attack, neoprene is less susceptible to attack from lubricants such as fluorocarbons (Teflon®), silicones, and petroleum-based lubricants; whereas lubricants (except, notably, vegetable-based lubricants) in contact with natural rubber for extended periods tend to migrate into the rubber.

Natural rubber can withstand the effects of low temperature better than neoprene. Due to increased stiffness with cold, neoprene is normally not employed in situations where the temperatures are likely to drop below -40°F, but natural rubber can be used in temperatures as low as -60°F. Both can be used to 180°F.

The above properties are important in predicting the longevity of the bearing under a guyed tower. It is difficult to determine the better of the two candidate elastomers. The manufacturer recommends use of natural rubber for the elastomer pad. Where natural rubber is employed, however, a vegetable-based lubricant must be used in the bearing interior between steel and elastomer. In addition, it is of the utmost importance to isolate the rubber by the impregnated foam and the elastomeric sealing band from the ozone-rich environment surrounding a VLF tower. The rubber used in the bearings should be made from natural rubbers and free from fillers except carbon black and zinc oxide which should be used in sufficient quantity to give the required hardness. An antiozonisant should be included for the rubber to conform to ASTM specification D-1149-55T. The rubber should have the following characteristics:

Hardness	50-55 Shore A durometer
Minimum tensile strength	2,700 psi
Minimum tear strength	285 psi
Elongation at break	600%
Maximum compression set	25% of original thickness in accordance with ASTM D-395 method B

The natural rubber bearing pad, with proper isolation and lubrication, should function without maintenance (except for the elastomeric band) for several decades.

PHASE II – LABORATORY LOAD TESTS

Laboratory loading tests were conducted on the Andre bearing shown in Figure 3 and a CEL-fabricated bearing shown in Figure 8a which employed geometry and material deviations from the manufacturer's product. Although tests by California's State Highway Department had demonstrated that the confined bearing was capable of withstanding cyclic, normal compression plus horizontal loading, the bearings were tested using static loading, simulating more extreme conditions. Three loading configurations were employed: (1) axial compression up to four times the design loading; (2) axial compression plus rotation beyond

that allowable by the design; and (3) axial compression, horizontal shear, and rotation with the piston plate bearing against the inside wall surface of the cylinder pot (cylinder plate plus cylinder wall). Figure 3a indicates bearing components.

The CEL-fabricated bearing was identical to the manufacturer's bearing in overall dimensions except as noted in the detail drawing of Figure 8b. The bearing plates were axisymmetric instead of square; the circumferential, angular edges of the piston plate were rounded with a mild radius. The plates employed work-hardened, high-strength* ASTM designation A588 steel. The two-piece piston/cylinder assembly was machined in a lathe with relative ease in about 10 hours. The same rubber elastomer used in the manufacturer's bearing was employed in the CEL-fabricated bearing. The recommended design load for the tested bearings was 100,000 pounds or approximately 3,500 psi applied to the elastomer pad. This working stress is well below 57,000 psi, which has been successfully applied to confined rubber elastomers without apparent damage.

During all tests the bearings were monitored by electrical strain gages and mechanical deflectometers. Four electrical strain gages were mounted to monitor tangential strain on the outside surface of the cylinder walls as shown in Figure 9. The mechanical deflectometers were positioned as shown in Figure 10.

Axial Compression Tests

The test arrangement for the axial compression tests is shown in Figure 10. Tests were conducted in Tinius-Olson 200,000- and 400,000-pound test machines. Loads up to 400,000 pounds were applied to the bearing (14,000 psi applied to the elastomer pad). Strain gage and deflectometer results are plotted in Figures 11a and 11b. Tangential strain in the cylinder walls averaged 60μ to 70μ**/100 kips in the manufacturer's bearing and 55μ/100 kips in the CEL bearing. This compares with 65μ/100 kips predicted by the finite element solution to be discussed in Phase III of this report. The elastomer pad was compressed only 0.0375 inch after the application of 400,000 pounds, no permanent set was detectable after load removal. This deflection represents an average compressive strain of 1.88% for each 100 kips of applied load. After 10 load cycles up to 400,000 pounds, the elastomer pads showed no damage.

Axial Compression Plus Rotation Tests

The test arrangement for axial compression plus rotation is shown in Figure 12. During the rotation tests, the bearing design load (100,000 pounds) was maintained while the bearing was rotated about its x- and y-axes, as defined in Figure 9. The constant compression load was applied in the testing machine while hydraulic jacks with hinged-end rams provided rotation (see Figure 12). By varying the ram lengths of the jacks but maintaining constant

*Steel strength = 50 ksi.

**$\mu = 10^{-6}$ in./in., or microstrains.

pressure, the bearings were rotated from the horizontal by ±1.4 degrees (1 in 40) and subjected to a constant compressive load of 100,000 pounds. Each hydraulic jack maintained an equal loading of 50 kips. The amount of rotation was limited by the piston plate's making contact with the top of the cylinder pot. The manufacturer's recommendation for limiting design rotation was 1 in 50.

The strain gages were monitored to determine variation of tangential strain in the cylinder wall while the elastomer was subjected to rotation and 100-kip compression. The maximum strain recorded was 150μ. During rotation, the strain did not vary more than 40μ from the mean value recorded in each gage. The mean values in each of the four gages measured at maximum loading varied from 75 to 110μ. As in other tests, these values are very low and are less than, or at most comparable to, the nominal compressive strain in the piston and cylinder plates (where the nominal compressive steel stress applied to the steel plates was approximately 2,000 psi).

After 20 rotation cycles the bearings were disassembled and inspected for damage. The piston stayed well-sealed on the elastomer rubber pad after the design load was applied, and the piston did not rub against the cylinder walls during rotation. Consequently, no apparent damage of the piston-cylinder assembly or the elastomer pad was detected.

Compressive and Horizontal Shear Tests

The test arrangement is shown in Figure 13 for applying compressive and horizontal shear loading on the bearings plus a constant rotation. Two strain gage alignments of shear direction and rotation with the x- and y-axes of each bearing were considered (see Figures 9 and 14 through 17). The first loading case had the shear force direction aligned with the y-axis plus 1-degree constant rotation about the x-axis. The second loading had the shear force direction aligned with the x-axis with 1-degree constant rotation about the y-axis. As the loading was applied to the bearings, the compression and shear were increased proportionately while the rotation (relative angle between top and bottom plates) remained constant at approximately 1 degree.

Strain gage results from the four tangential gages are plotted in Figures 14 through 17. The alignment of the gages with the shear loading is given in each figure. Maximum tangential strain at the design compressive load was 500μ to 600μ for the Andre bearing and approximately 250μ for the CEL bearing. The strain was tensile, and the maximum value usually occurred on the side adjacent to the point where the piston bore against the cylinder wall due to horizontal shear loading. At the position opposite to where the piston bore against the cylinder wall, the load-strain relationship was nonlinear.

After 10 cycles of compression-shear-rotation in each of the two alignments, the bearings were disassembled and inspected; the rubber elastomer showed no effect from the tests. However, on the manufacturer's bearing, scouring was found on the cylinder wall (Figure 18) and the angular, circumferential edge of the piston was scoured and rounded slightly (Figure 19) from the piston's bearing against the cylinder due to rotation and

horizontal shear loading. The positions on the piston and cylinder wall are identified by points A and B, respectively, in Figure 3. This scouring did not occur in the CEL-fabricated bearing in the piston and cylinder because the circumferential edges of the hardened steel piston were rounded during machining. The CEL bearing with its changes in geometry and use of work-hardened steel proved to be superior to the manufacturer's bearing by decreasing the strain in the cylinder wall and eliminating scouring of the cylinder due to horizontal shear plus rotation.

PHASE III – FINITE ELEMENT STUDY

Finite element analyses were performed on the CEL-modified configuration of the encased rubber bearing using WILREL [14] and AXS [15], two axisymmetric geometry stress-analysis programs. The following material properties were employed:

Steel:	Young's Modulus – 30×10^6 psi
	Poisson's Ratio – 0.30
Elastomer:	Young's Modulus – 1,000 psi
	Poisson's Ratio – 0.48

The finite element model consisted of the cylinder plate with the cylinder walls and the elastomer pad. The piston plate was not modeled (discretized) but was assumed to load the elastomer pad uniformly in compression. The finite element mesh with element numbers of the bearing cross section (without piston) is shown in Figure 20. The element mesh was generated using the mesh generation subroutine of the main programs. The bearing cross section was discretized with straight lines, with a finer mesh on the surface of the cylinder wall to better predict the local stress concentrations which were expected in those areas. The mesh of the finite element model consisted of 96 elements.

In the WILREL program, the rubber pad was loaded in uniform compression of 1,000 psi as by the piston plate in the first load case of the laboratory tests. The stress results presented herein are in terms of 1,000-psi loading; and, as a result, a factor, equal to the pressure magnitude in ksi applied to the bearing, must be used to extrapolate the results to higher loadings. Stress contour plots from the WILREL solution are shown in Figures 21 through 24, presenting the vertical, radial, tangential, and maximum shear stress plots, respectively. The compression loading resulted in no areas of excessive stress magnitude. The maximum tensile stress of 1,257 psi (1.257 times the applied loading) occurred in element 61 located on the inside surface of the cylinder plate at its intersection with the cylinder wall (see Figure 20). The maximum compressive stress was equal to the applied load (1,000 psi) and occurred in the lower plate. All other stress components were of less magnitude than the applied loading. Maximum tensile stress in the cylinder wall was 674 psi on the inside surface (elements 47 and 48). The maximum compression in the cylinder was a radial

component near the interface of the elastomer and the cylinder wall and equalled the applied pressure. In general, maximum stresses in the elastomer equalled the applied pressure as expected. Vertical stresses in the cylinder plate were of significantly higher magnitude than the circumferential and tangential stresses.

The tangential strain in the cylinder surface element at the location comparable to the position of the electrical strain gage in the laboratory tests is plotted in Figure 11 for comparison with the strain gage results. The finite element results agree with the strain gages within 20%.

The AXS program allows nonaxisymmetric loading on an axisymmetric solid using summation of even terms from a Fourier series to represent the loading [15]. The finite element model was subjected to a horizontal load applied against the inside of the cylinder wall on the surface nodes of element 48. This was to represent the piston bearing against the cylinder when the bearing is subjected to horizontal shear. The loading is shown in Figure 25. This loading arrangement assumes the elastomer's resistance to shear is negligible, compared to the resistance of the cylinder wall. The stress intensities were checked in the cross section where the loading was applied as well as in the cross sections at 15, 30, 90, and 180 degrees from the point where the load was applied. The magnitude of the total shear force equalled 3,000 pounds or approximately one-tenth the total compressive force applied in the WILREL analysis.

Maximum stresses occurred in the cross section at the point of load application. The contours for the vertical, radial, tangential, and maximum shear stresses for this cross section are presented in Figures 26 through 29, respectively.

In the cylinder wall the maximum compressive stress was 32,400 psi and was located on the inside surface of the cylinder at the point of application of the horizontal load. The maximum tensile stress in the cylinder wall was a tangential component equal to 12,600 psi occurring in element 9 on the outside surface. The maximum tensile stress in the model for the horizontal shear load case was 22,000 psi occurring in element 61 located on the inside surface of the bottom plate at the intersection of the cylinder wall. Stresses in the bottom plate away from the cylinder wall were not appreciably high due to the location of the applied horizontal shear load.

The values of the tangential strain in element 12, corresponding to the position of the strain gages in the laboratory tests, were algebraically summed with the strain from the same element in the WILREL solution. These results for various cross sections (which are identified) are plotted in Figure 30 for comparison with the strain gage results from the compression, horizontal shear, and rotation tests (Figures 14 through 17). The finite element results bracketed the strain gage results: that is, the strain gages measured about 50% higher strains than the lowest tensile strain predicted by the finite element analysis, but the strain gage results were almost 50% lower than the highest tensile strains from the finite element analysis. In general, the stresses were not excessive in the bearing configuration except at the point at which the piston is expected to bear against the cylinder wall during application of horizontal shear loading. By making the diameter of the piston as close as possible to the diameter of the cylinder, these stresses can be greatly reduced.

Table 2. Candidate Elastomeric Materials for Outer Clamp-On Band to Seal Antenna Elastomeric Bearing Hinge (Elastomers chosen are compatible with silicone oils and greases.)

Properties [17]	Characteristics of Following Elastomers —			
	Fluorosilicone	Ethylene Propylene Diene	Chlorosulfonated Polyethylene	Fluorocarbon
Tensile strength, psi (block loaded stocks)	<2,000	800-3,200	1,500-2,500	1,500-3,000
Elongation, reinforced, %	200-400	200-600	250-500	100-450
Flex cracking resistance				
Slow rate	good	good	good	good
Fast rate	good	good	good	good
Tear strength	fair	poor-fair	fair-good	poor-fair
Abrasion resistance	poor	good	excellent	good
Electrical insulation	good	very good	good	good
Service temperature, °F				
Minimum for continued use	-90	-60	-40	-10
Maximum for continued use	400	<350	<325	<500
Corrosion resistance				
Weather	excellent	excellent	excellent	excellent
Oxidation	excellent	excellent	excellent	outstanding
Ozone	excellent	excellent	excellent	excellent
Radiation	good	excellent	excellent	excellent
Water	excellent	good-excellent	good	good
Typical trade names	Silastic® Brand Fluorosilicone Rubber	Nordel®	Hypalon®	Viton®
Manufacturer	Dow Corning	DuPont	DuPont	DuPont
Cost/lb, uncompounded	$20-22	$0.48	$0.75	$11.00

RECOMMENDATIONS

The final determination of the suitability of the totally encased elastomeric bearing as a hinge joint at the base of large guyed towers can only be made after a trial installation at an existing tower. Tests and analyses by CEL and others have indicated that the Andre bearing with modifications can be employed as hinge joints in antenna towers. It appears that such a bearing can be constructed for less than $5,000 [16] (considerably less than the cost of a steel, spherical joint).

The recommended elastomer bearing configuration for a 3-million-pound guyed tower is shown in Figure 31. Essentially, the configuration dimensions were scaled up from the two bearings evaluated in this project. The required elastomer area to support 3-million pounds at 3,500 psi was provided by a 33-inch-diameter elastomer pad. The thicknesses of the cylinder wall, cylinder plate, and piston are more than adequate to resist the applied loading. The relatively large radius to round the circumferential edge of the piston plate as well as the 0.01-inch differential in the diameters of cylinder wall and the piston is required to reduce the contact stresses when the piston bears against the cylinder wall. According to Hertz theory [13], the contact stress will be 75 to 100 ksi upon the application of a horizontal shear load of 300,000 pounds (one-tenth total compressive load) as the tolerance between the piston and cylinder wall varies from 0 to 0.1 inch. Therefore, a high-yield-strength, quenched and tempered alloy steel with a yield strength in excess of 100 ksi should be used to fabricate the piston and the cylinder walls. Note that the cylinder wall and plate can be machined in two pieces and bolted or welded together since stresses (except for contact stresses) predicted by the finite element analysis are very low in the material. Likewise, the piston and upper plate can be prepared in two sections using high yield strength steel.

The top surface of the piston plate and the bottom surface of the cylinder plate should be machined to a 125 rms tolerance. All interior steel surfaces of the bearing assembly should be machined to a 125 rms tolerance. All exposed steel surfaces should be zinc metallized.

Four split sealing rings made of brass (1/16-inch thick and 3/4-inch wide, similar in geometry to those obtained from the bearing manufacturer) should be placed as shown in Figure 31 to prevent extrusion of the elastomer between the piston and cylinder wall. The split lines of the sealing rings should be offset 90 degrees relative to each other.

When the hinge bearing is assembled, the elastomer should be entirely coated with a lubricant that will have no adverse effect on the elastomer. The selection of this lubricant will depend on the elastomer employed. The piston and cylinder assembly should be sealed internally with a heavy polyurethane foam impregnated with bitumen (a special solution of petroleum resins, isobutylene, and isoprene).

The bearing should be sealed externally with an elastomeric band circumventing the bearing as shown in Figure 31. Four candidate materials for the band are listed in Table 2; chlorosulfonated polyethylene is recommended. This material should be serviceable for approximately 15 years before replacement is required. Stainless steel clamps can hold the elastomeric band in place.

Table 3. Candidate Elastomeric Materials for Internal Bearing Pad for Elastomeric Hinge Bearing

Properties[a]	Characteristics of Following Elastomers –	
	Natural Rubber (black)	Neoprene
Tensile strength	3,500-4,500 psi	3,000-4,000 psi
Elongation	580-650%	500-600%
Tear resistance	excellent	fair to good
Abrasion resistance	excellent	good
Sunlight aging	poor	very good
Oxidation resistance	good	excellent
Heat aging	good	excellent
Minimum recommended serviceable temperature	-60°F	-40°F
Maximum recommended serviceable temperature	180°F	240°F
Water-swell resistance	fair	fair to excellent
Rebound		
Cold	excellent	very good[b]
Hot	excellent	very good[b]
Compression set [7]	good	fair to good
Ozone resistance [7]	fair	excellent
Resistance to silicone oils and greases	some leaching out of carbon black[c] excellent to silicone-based hydraulic oil [18]	excellent to silicone-based hydraulic oil [18]
Resistance to GE Versilube silicone lubricants [19]	-40° to 180°F, use low plasticizer compounds only	-40° to 200°F

[a]Unless otherwise stated, properties listed are from Reference 17.

[b]92% of natural rubber.

[c]Telephone conversation between author and technical representative from Dow Corning Corporation.

The elastomer material for the bearing pad of the assembly shown in Figure 31 was considered in detail. The two elastomers most commonly employed in similar bearing applications in bridge construction are natural rubber and neoprene (chloroprene). Relevant material properties of these two elastomers are presented in Table 3. The most important properties for the elastomer in the hinge bearing are as follows: (1) low temperature stiffening, (2) compression creep, (3) load deflection or stress compression, and (4) aging properties.

ACKNOWLEDGMENTS

Stanley K. Takahashi initiated the project at CEL. The author was assisted by V. Gerwe and D. Corrente, structural engineering technicians, and R. Cooper, engineering technician.

REFERENCES

1. Naval Facilities Engineering Command. Memo Code 041 to Code PC6 of 18 Jun 1973. Subj: Ball joint base hinge for Annapolis and Lualualei VLF towers.

2.———. Memo Code 041 to Code PC6 of 14 Mar 1973. Subj: Lualualei VLF towers; jacking problems associated with foundation stress and ball joint lubrication and alignment recommendations.

3. F. Leonhardt and W. Andre. "New developments concerning bearings," Special publication from Die Bautechnik, vol 39, no. 2, 1962, pp 37-50.

4. California Department of Public Works, Division of Highways. No. M&R 646142-1: Laboratory and field performance of elastomeric bridge bearing pads, by E. F. Nordlin, J. R. Stoker, and R. R. Trimble. Sacramento, CA, Jan 1968.

5. State of Illinois Department of Public Works and Buildings, Division of Highways, Bureau of Research and Development. Project no. IHD-7: Interim report of TFE expansion bearing for highway bridges, by F. K. Jacobsen and R. K. Taylor. IL, Jun 1971.

6. California Department of Public Works, Division of Highways. No. M&R 646142-2: Laboratory investigation of tetrafluoroethylene (TFE) as a bridge bearing material, by E. F. Nordlin, J. F. Bass, and R. R. Trimble. Sacramento, CA, Jun 1970.

7. E. I. Dupont de Nemours & Co., Inc. Elastomer Chemicals Department. Engineering guide to the Dupont synthetic rubbers. Wilmington, DE, Nov 1969.

8. C. E. Rejcha. "Elastomeric bridge bearings," Civil Engineering—ASCE, vol. 42, no. 5, May 1972.

9. Holmes and Narver, Inc. 1200-ft Annapolis tower, Lapp insulators redesign, computer printout for tower analysis. Anaheim, CA, Jan 1972.

10. F. M. Fucik, J. E. Goodman Sales Limited, Chicago ltr to Illinois Department of Public Works and Buildings, Division of Highways of 5 Jul 1967.

11. F. G. Tatnall. "Development of the scratch gage," Experimental Mechanics, vol 9, no. 6, Jun 1969, p. 27N.

12. F. M. Fucik, J. E. Goodman Sales Limited, Chicago ltr to E. L. Mifflin, NAVFAC Code 0412 of 27 Mar 1973.

13. Fel-Pro, Incorporated. Elastomeric bearings design and specification manual. Skokie, IL, 1972.

14. E. L. Wilson. "Structural analysis of axisymmetric solids." American Institute of Aeronautics and Astronautics Journal, vol 8, no. 12, Dec 1965.

15. University of California, Earthquake Engineering Research Center. Report No. EERC-69-10: Dynamic stress analysis of axisymmetric structures under arbitrary loadings, by S. Ghosh and E. Wilson. Berkeley, CA, Sep 1969.

16. J. S. Elder, Andre Rubber Company (Canada) Limited ltr to S. K. Takahashi, Civil Engineering Laboratory, Port Hueneme of 30 Dec 1974.

17. "Materials selector 74," Materials Engineering, vol 78, no. 4, Sep 1973, pp 298-300.

18. D. J. Kelly. "Resistance of materials to hydraulic fluids," Machine Design, vol 43, no. 2, 21 Jan 1971, pp 100-103.

19. General Electric, Silicone Products Department. Technical Data Book S-10B: Versilube® silicone lubricants. Waterford, NY.

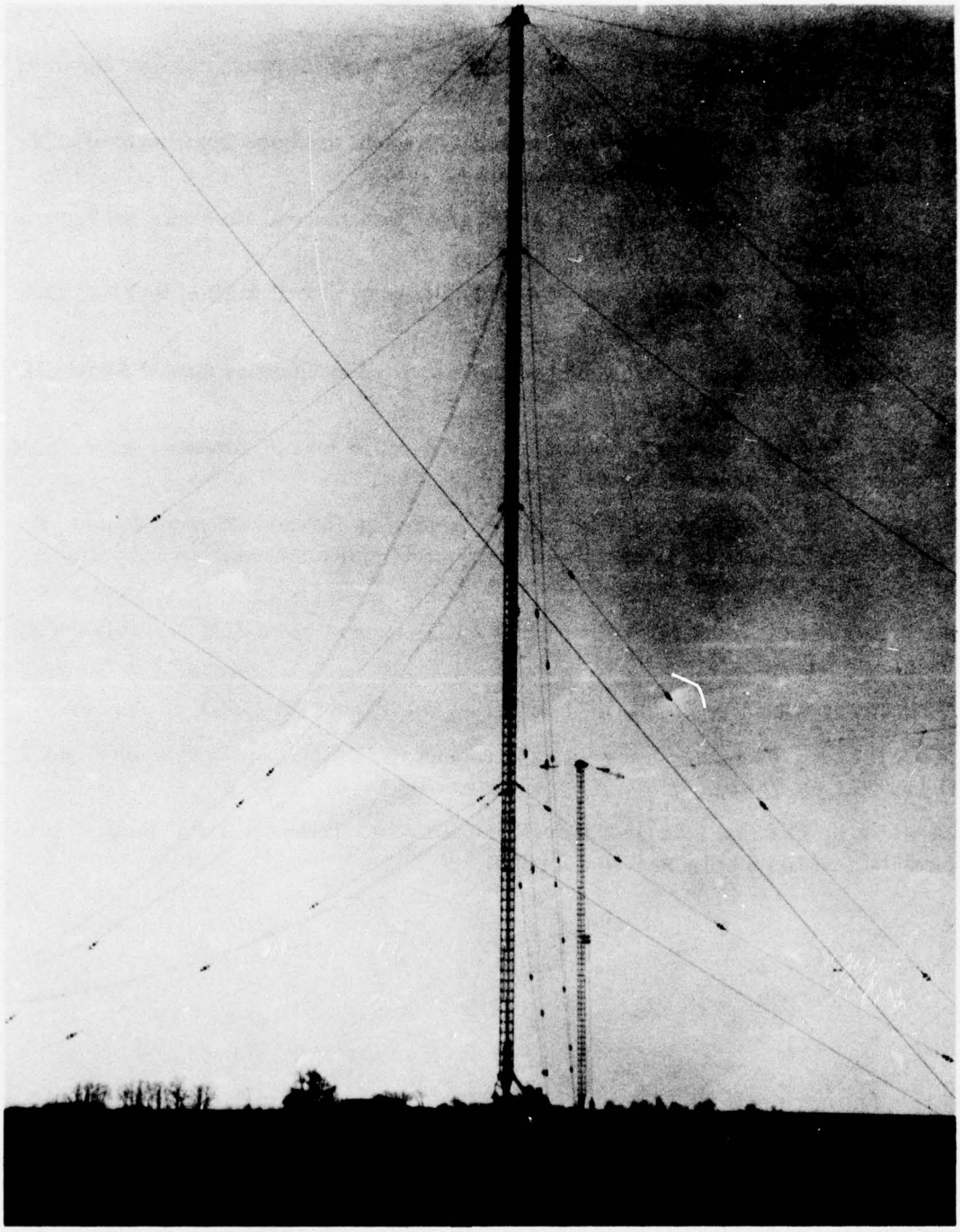

Figure 1. VLF antenna tower structure at Annapolis, Maryland.

(a) Overall.

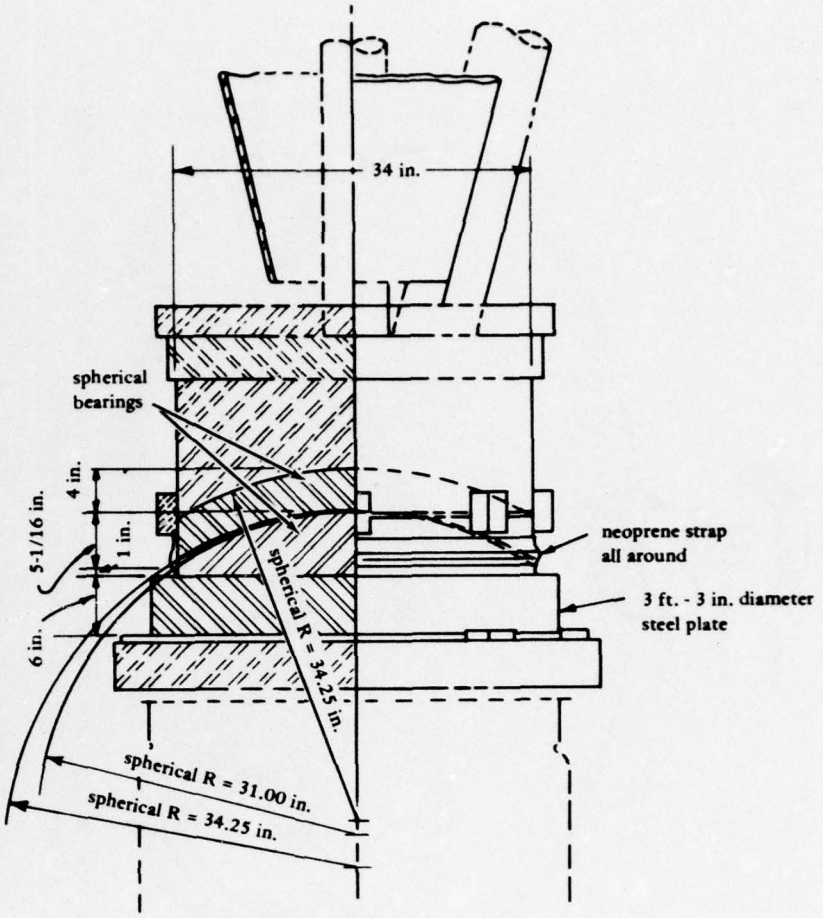

(b) Detail.

Figure 2. Spherical bearing hinge at Annapolis, Maryland.

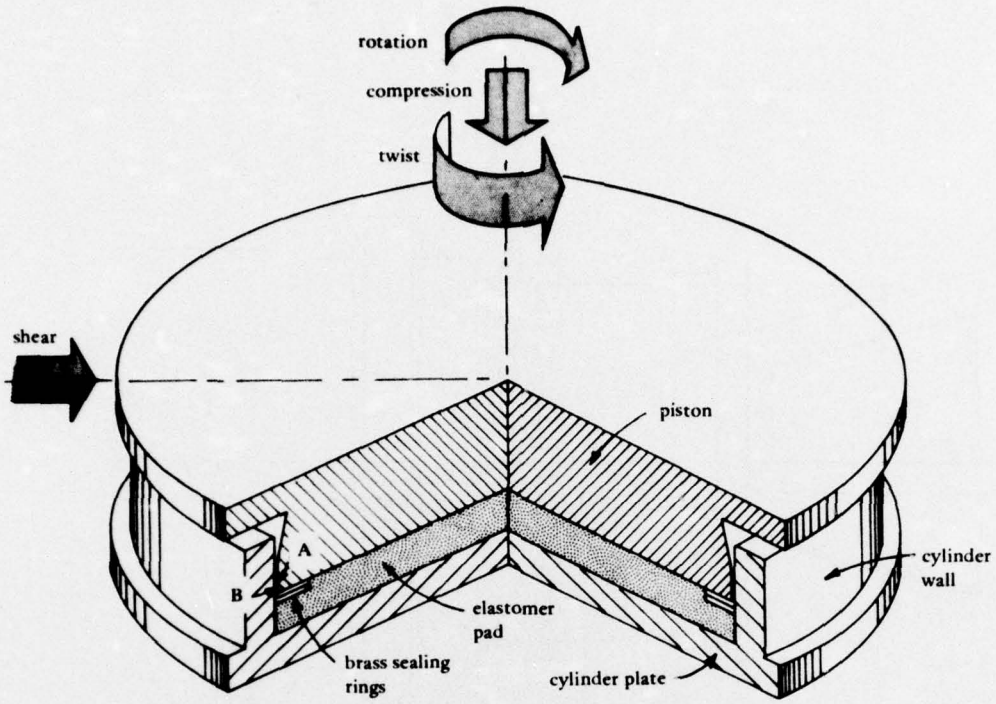

(a) Cutaway view showing components and applied mechanical loading and action. A is point of scouring on piston wall; B is point of scouring on cylinder wall.

(b) Andre elastomer bearing assembly.

Figure 3. Totally encased elastomeric bearing configurations.

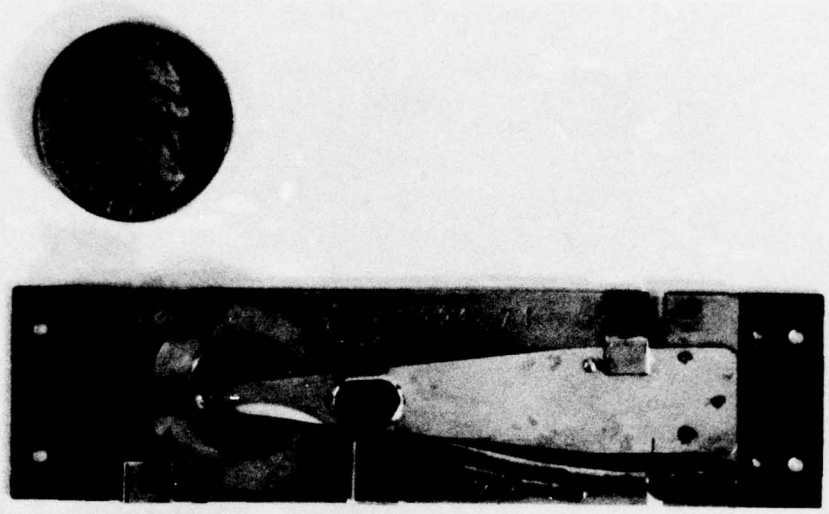

Figure 4. Three-inch scratch gage.

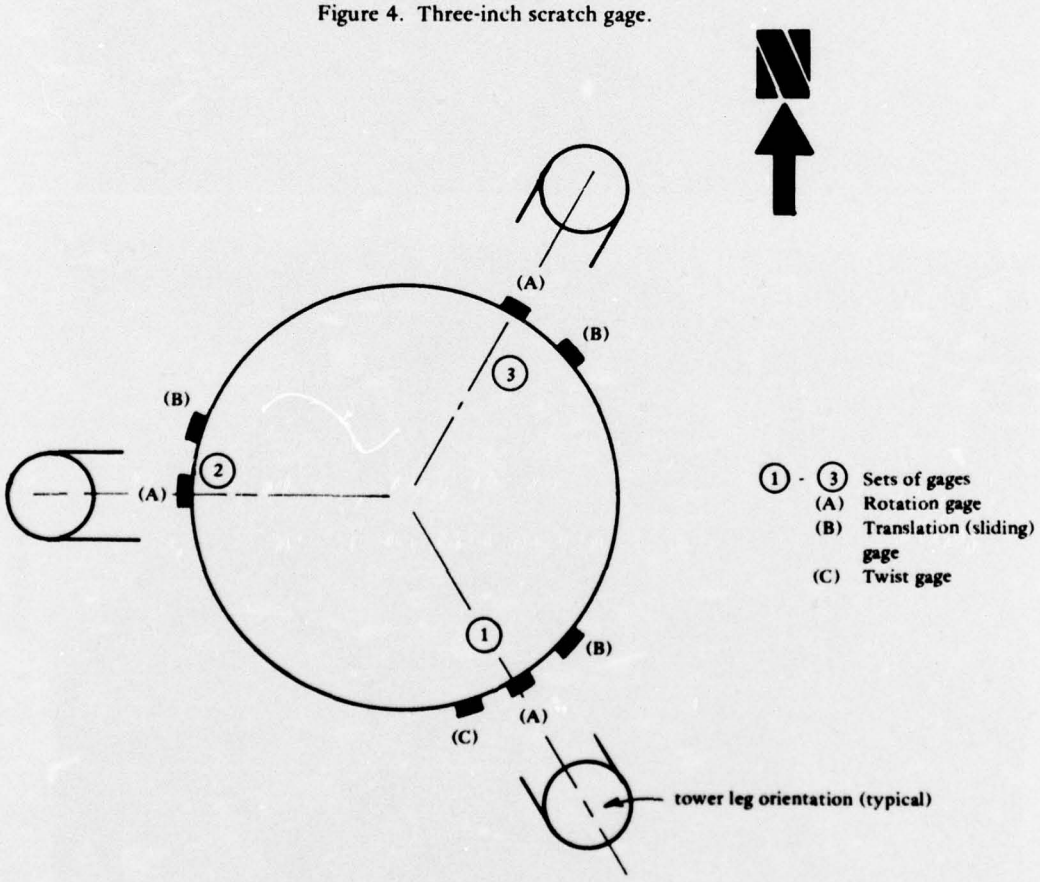

Figure 5. Bearing hinge plan, showing scratch gage locations.

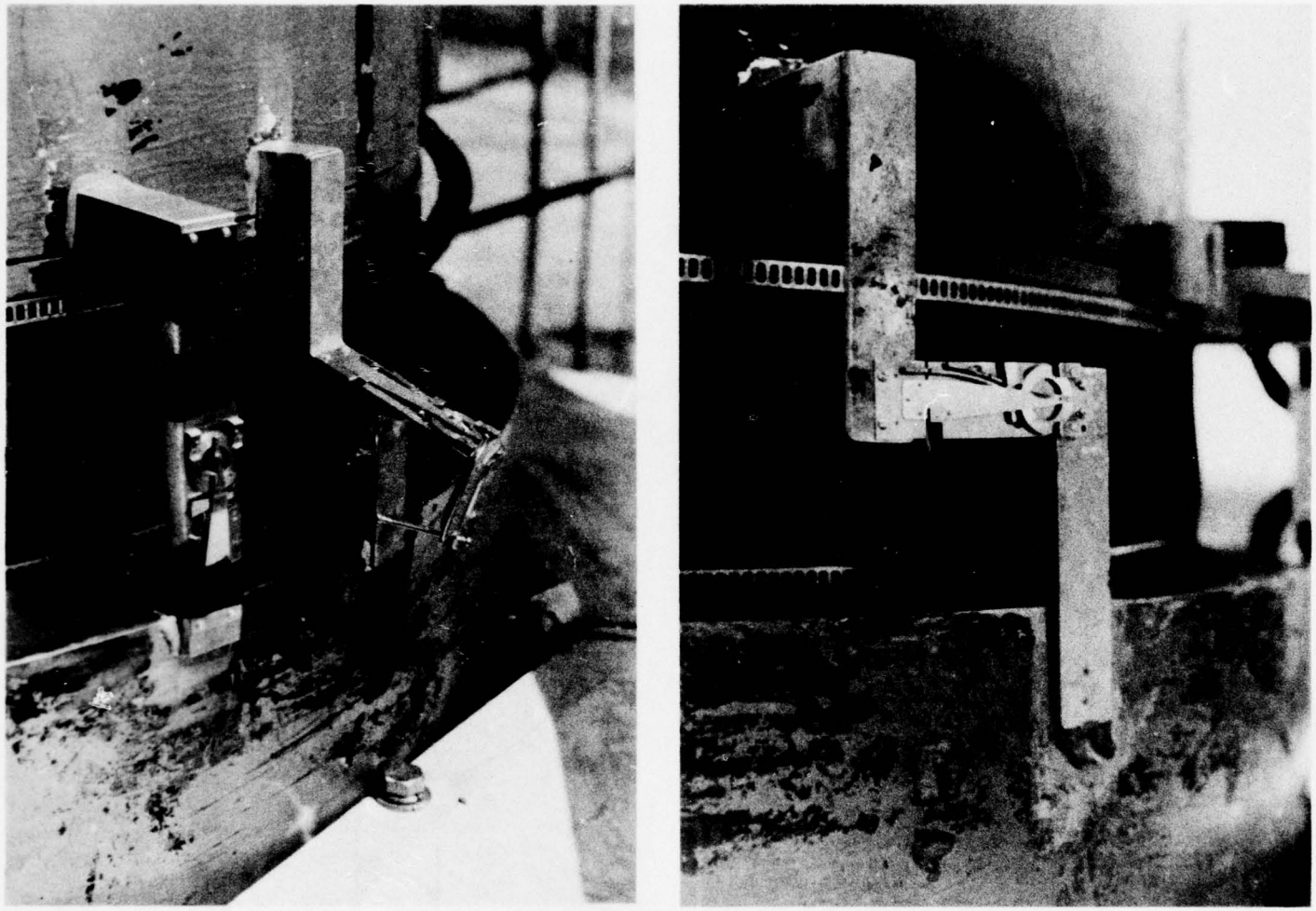

(a) Gages (A) and (B).

(b) Gage (C).

Figure 6. Scratch gages mounted on Annapolis VLF tower.

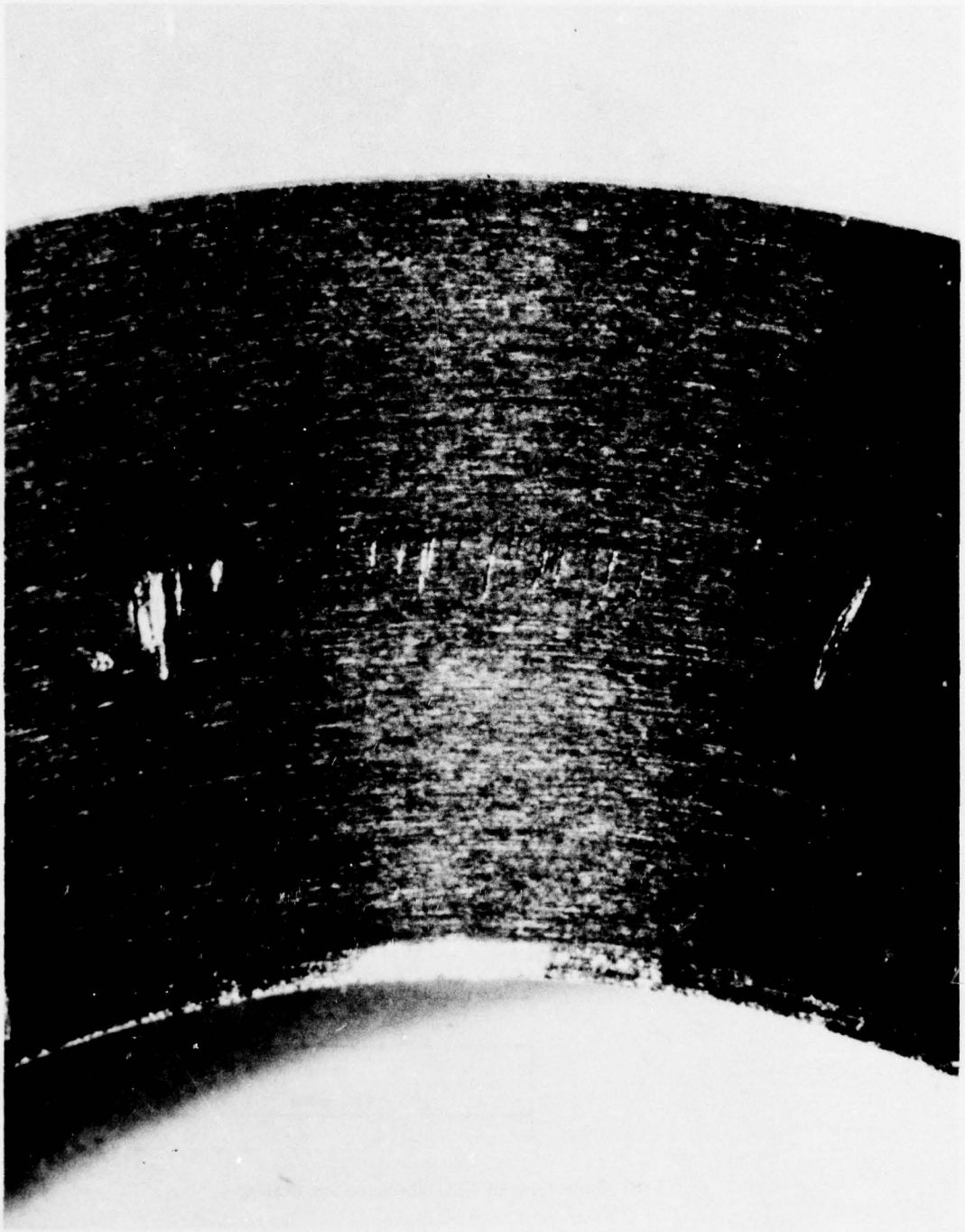

Figure 7. Scribe recording from scratch gage located to measure rotational movement.

(a) Piston plate and cylinder pot.

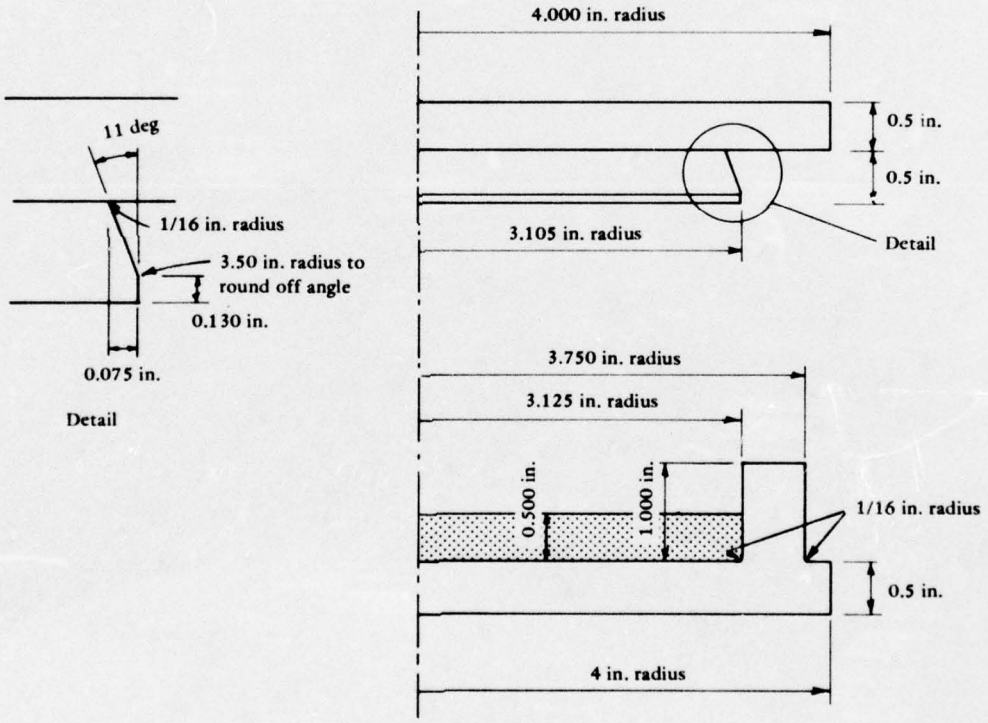

(b) Dimensions of CEL-fabricated test bearing.

Figure 8. CEL-fabricated test bearing.

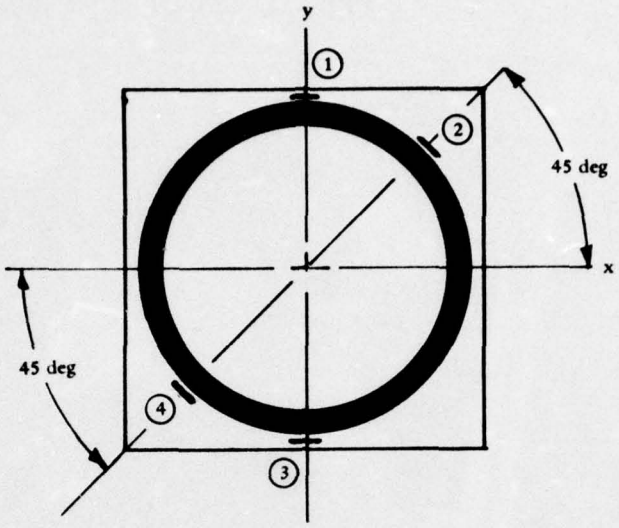

(a) Andre bearing pot.

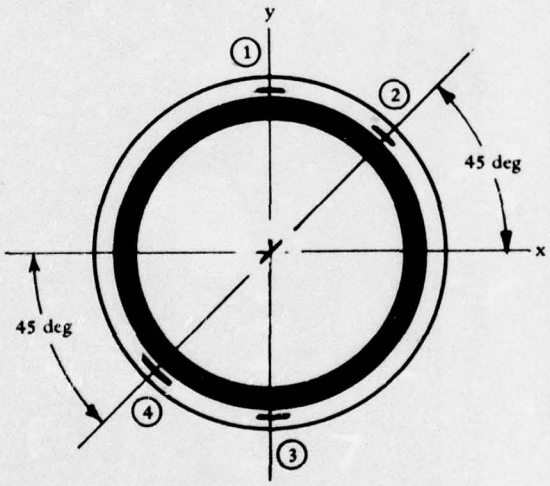

(b) CEL-fabricated pot.

Figure 9. Plan view of strain gage locations on cylinder walls of bearing pots.

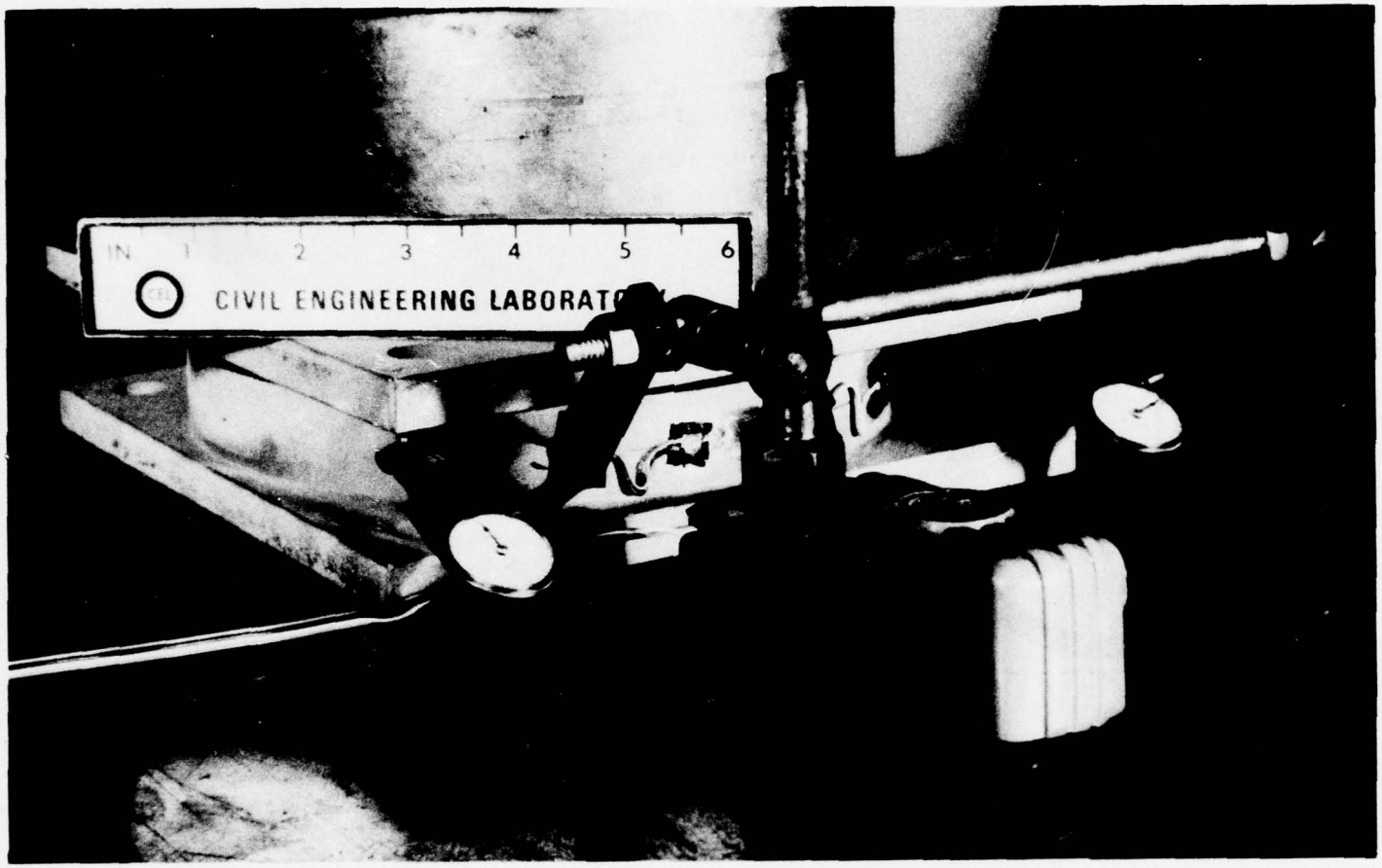

Figure 10. Elastomeric bearing assembly during compression test.

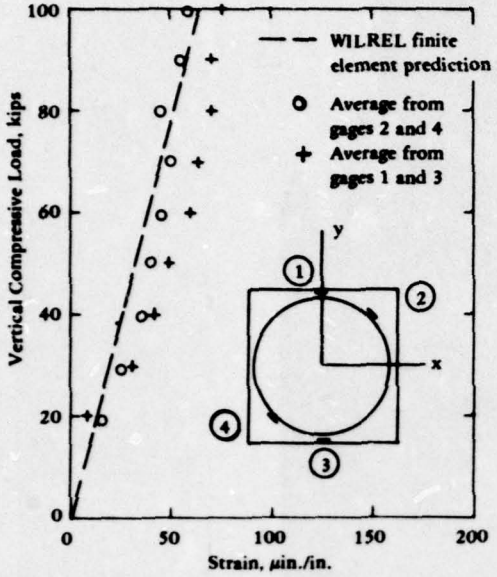

(a) Tangential (hoops) strain on exterior surface of pot cylinder; Andre bearing subjected to axial compression.

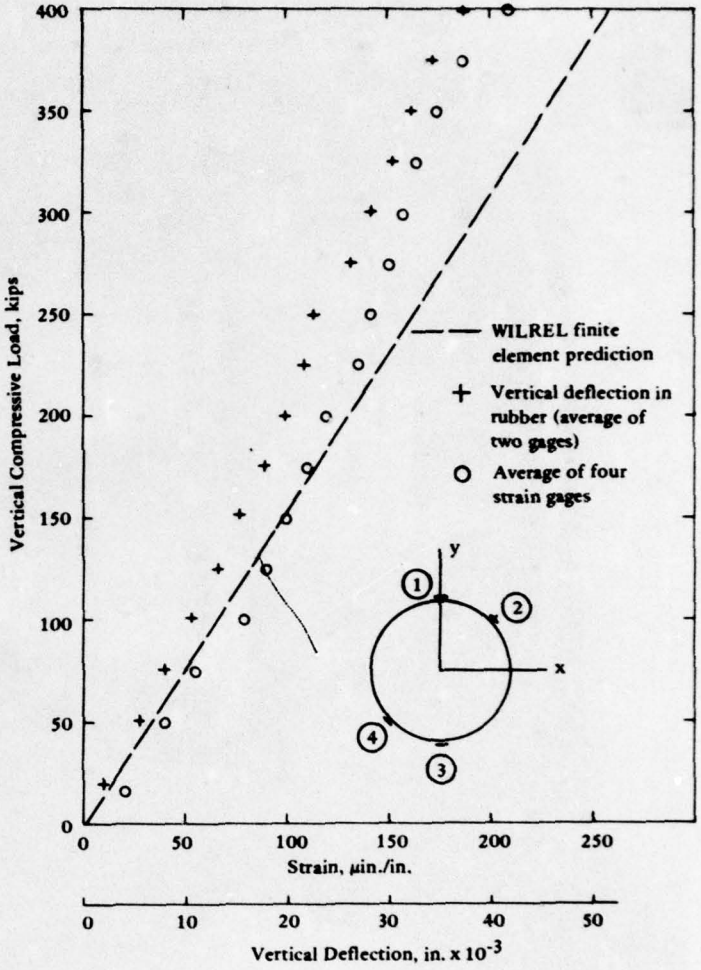

(b) Vertical deflection and exterior tangential strain on pot cylinder; CEL bearing subjected to axial compression.

Figure 11. Deflection and strain gage results from bearing compression tests.

Figure 12. Compression and rotation test setup.

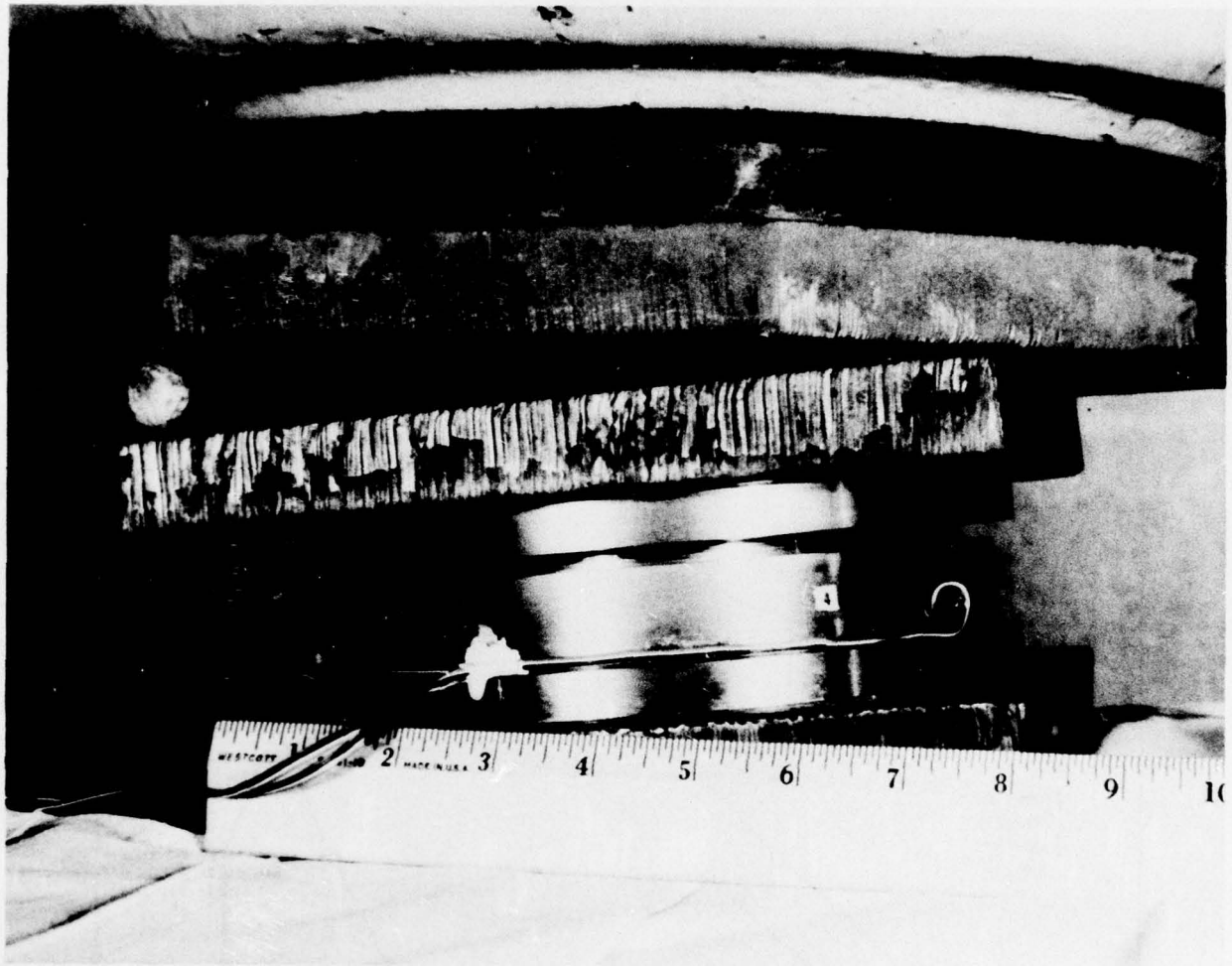

Figure 13. Setup for compression, horizontal shear, and rotation tests.

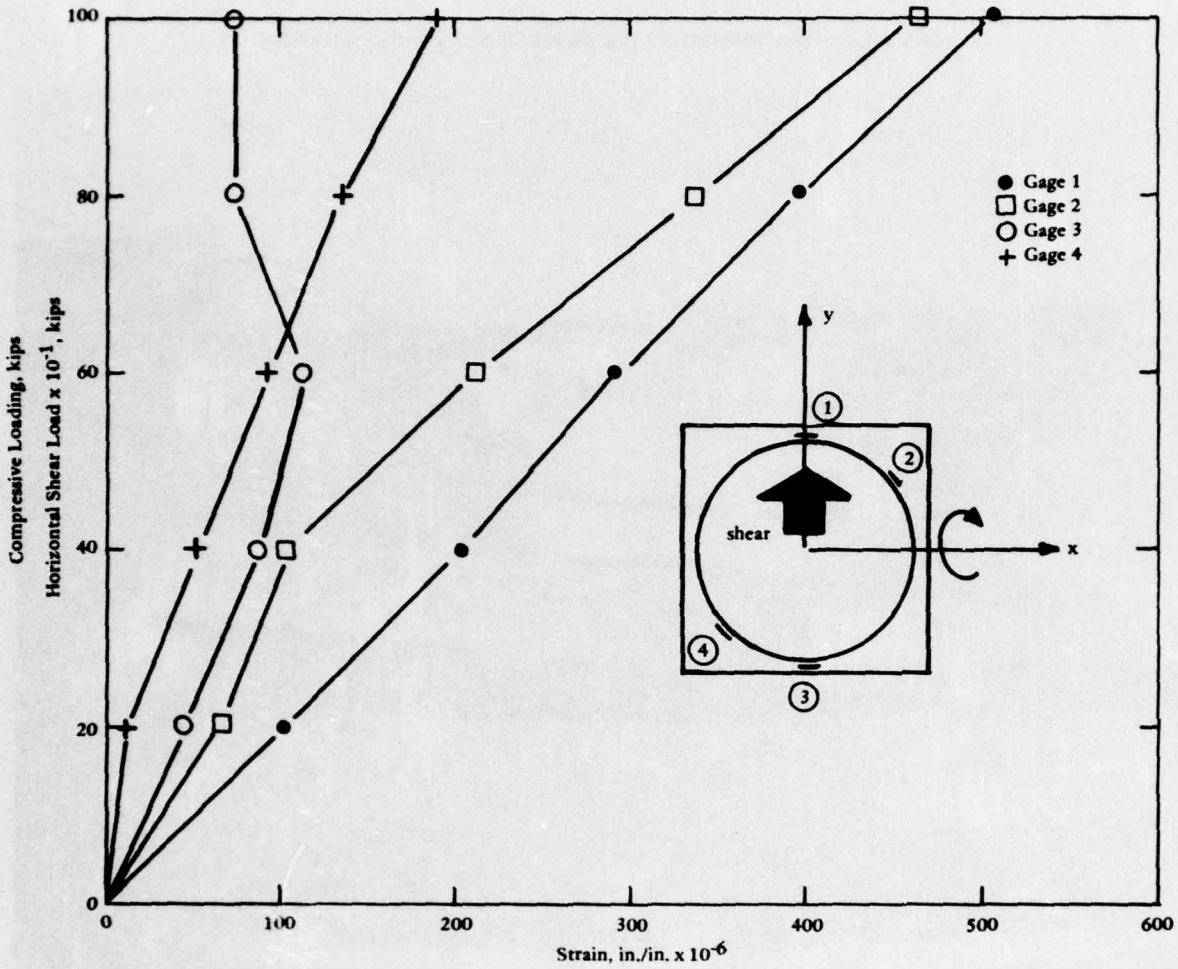

Figure 14. Andre bearing strain gage readings: compression with horizontal shear (one-tenth the compression load) in the y-direction and 1-degree rotation about the x-axis.

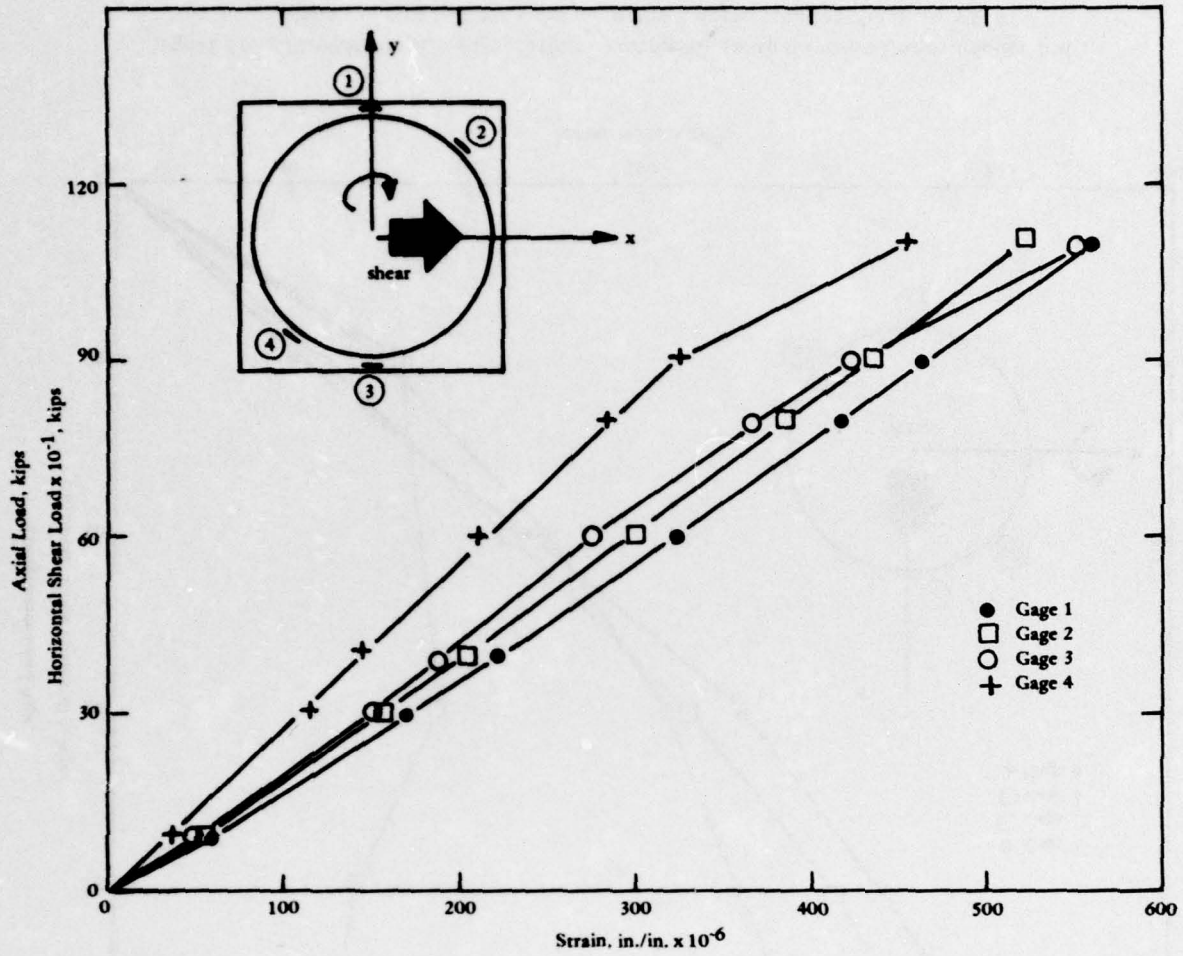

Figure 15. Andre bearing strain gage readings: compression with horizontal shear (one-tenth the compression load) in the x-direction plus 1-degree rotation about the y-axis.

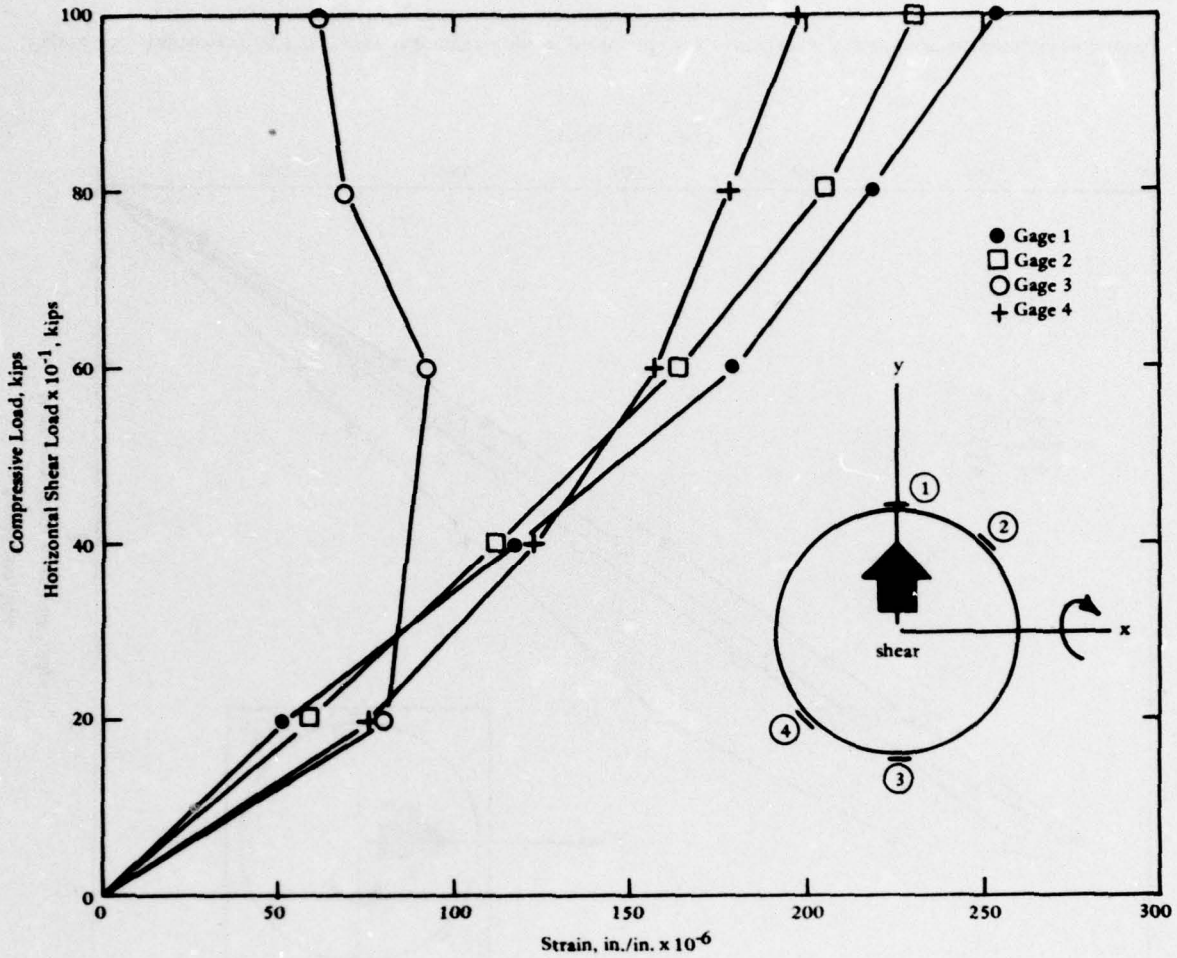

Figure 16. CEL bearing strain gage readings: compression with horizontal shear (one-tenth the compression load) in the y-direction plus 1-degree rotation about the x-axis.

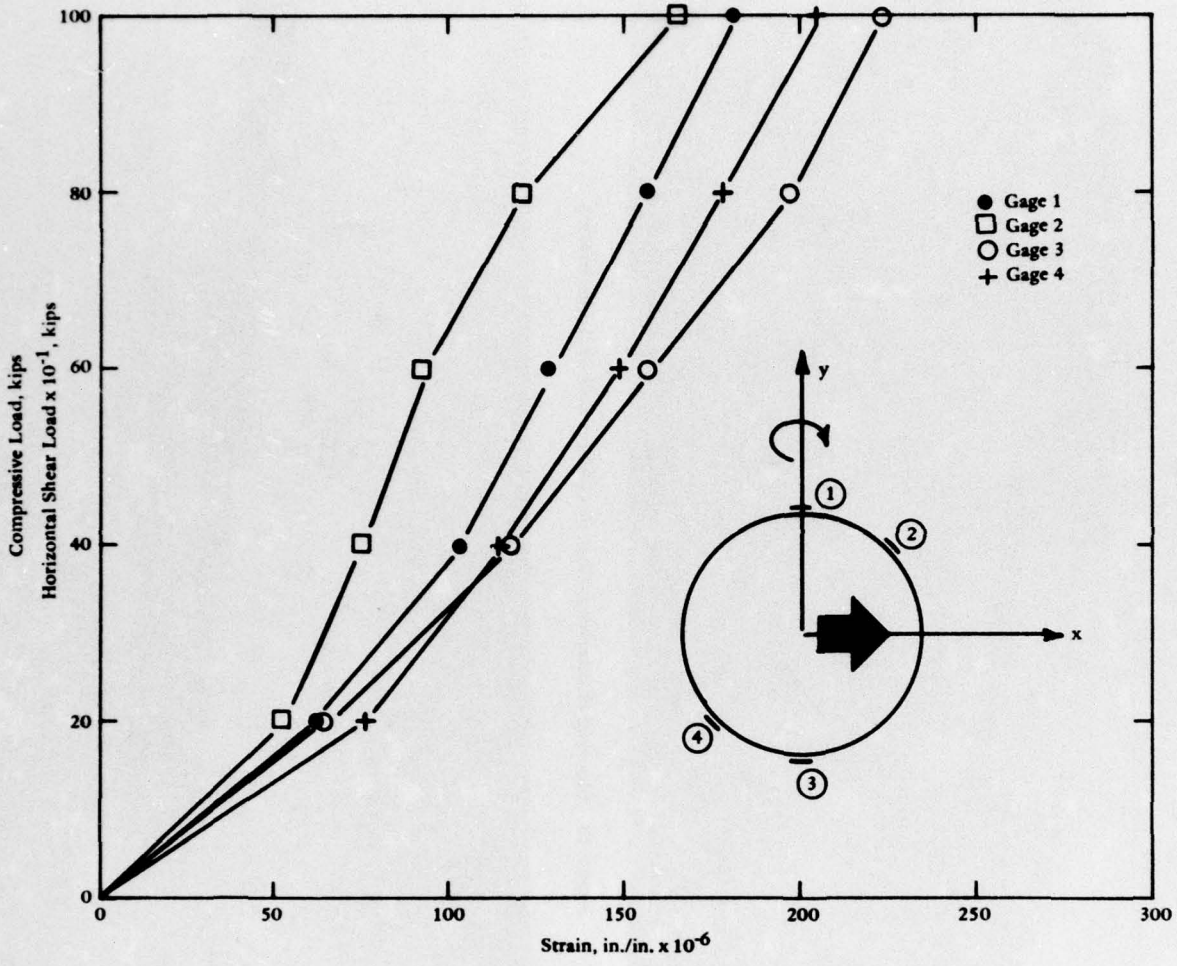

Figure 17. CEL bearing strain gage readings: compression with horizontal shear (one-tenth the compression load) in the x-direction plus 1-degree rotation about the y-axis.

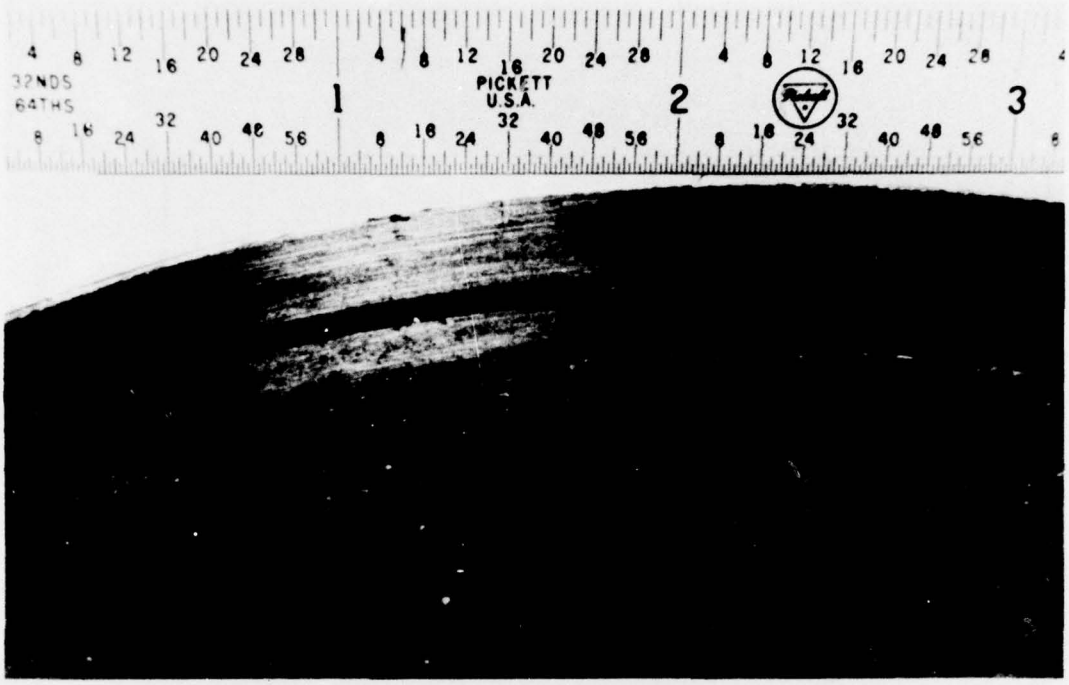

Figure 18. Scouring of interior surface of cylinder wall of Andre bearing.

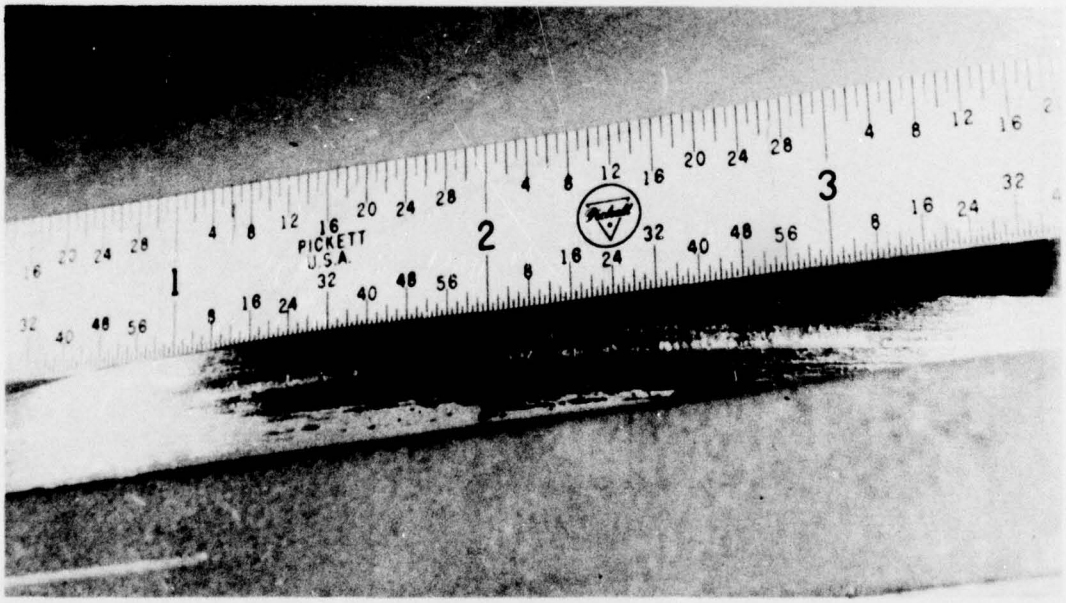

Figure 19. Scouring of piston circumference of Andre bearing.

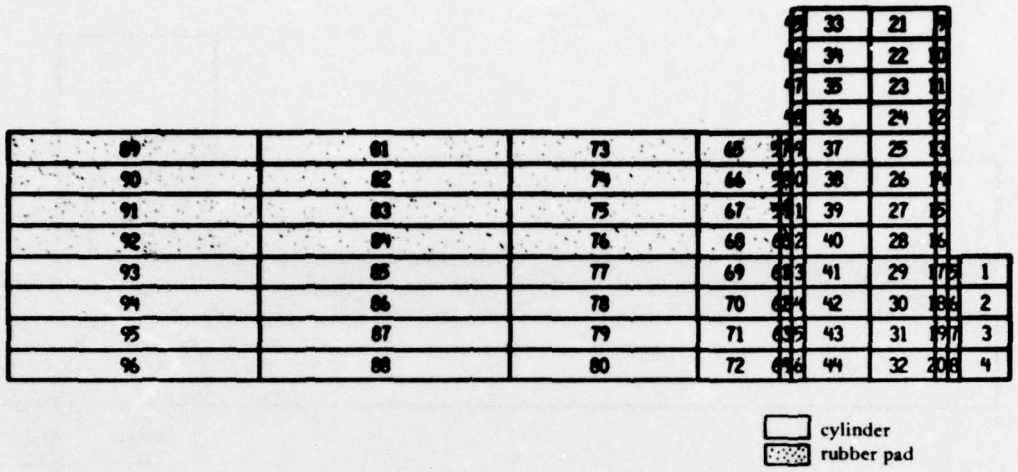

Figure 20. Finite element mesh and element numbers for bearing tests.

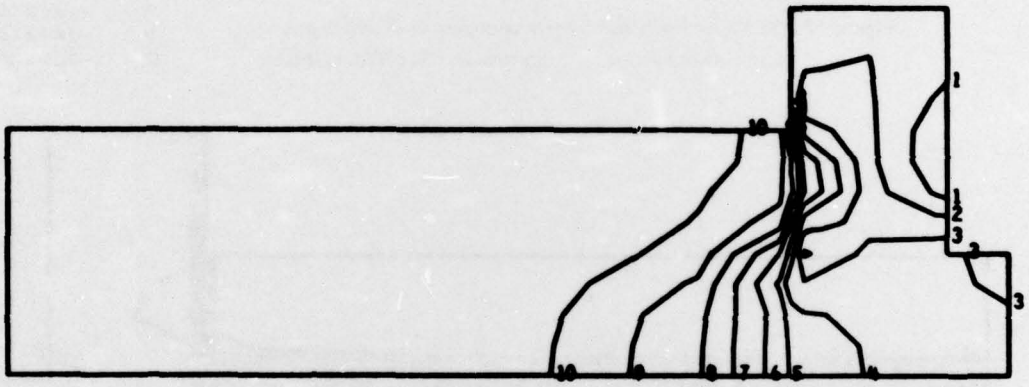

Contour No.	Stress (psi)
1	1.04×10^{02}
2	-6.79×10^{00}
3	-1.17×10^{02}
4	-2.28×10^{02}
5	-3.39×10^{02}
6	-4.50×10^{02}
7	-5.61×10^{02}
8	-6.72×10^{02}
9	-7.82×10^{02}
10	-8.93×10^{02}

Figure 21. Vertical stress contours in cylinder pot and elastomer with uniform compression load of 1,000 psi on rubber pad (WILREL solution).

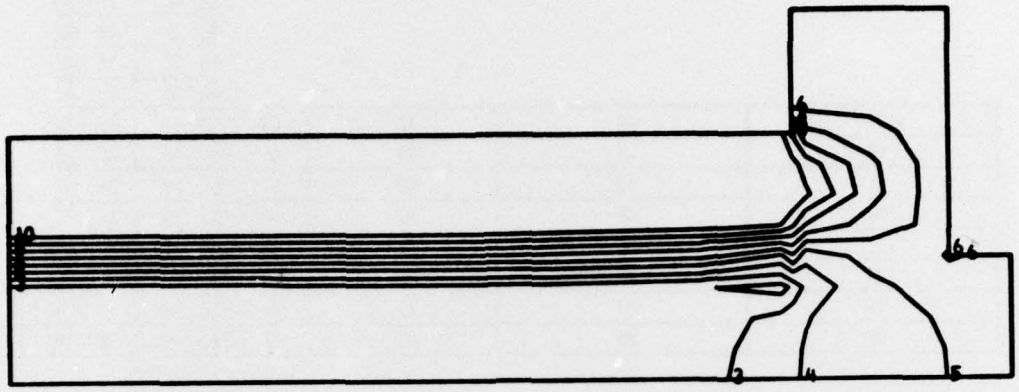

Contour No.	Stress (psi)
1	6.61×10^{02}
2	5.05×10^{02}
3	3.49×10^{02}
4	1.94×10^{02}
5	3.84×10^{01}
6	-1.17×10^{02}
7	-2.72×10^{02}
8	-4.28×10^{02}
9	-5.84×10^{02}
10	-7.39×10^{02}

Figure 22. Radial or horizontal stress contours in cylinder pot and elastomer due to compression (WILREL solution).

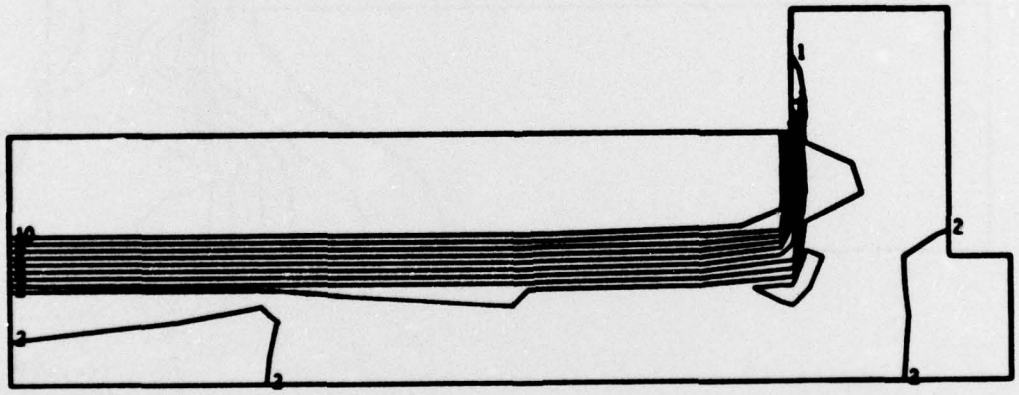

Contour No.	Stress (psi)
1	6.49×10^{02}
2	4.95×10^{02}
3	3.42×10^{02}
4	1.88×10^{02}
5	3.44×10^{01}
6	-1.19×10^{02}
7	-2.73×10^{02}
8	-4.27×10^{02}
9	-5.80×10^{02}
10	-7.34×10^{02}

Figure 23. Tangential stress contours in cylinder pot and elastomer due to compression (WILREL solution).

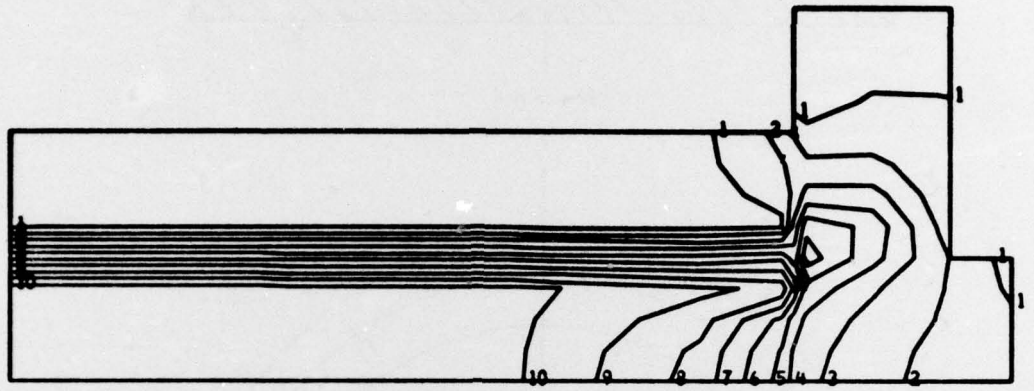

Contour No.	Stress (psi)
1	7.38×10^{01}
2	1.44×10^{02}
3	2.16×10^{02}
4	2.87×10^{02}
5	3.58×10^{02}
6	4.29×10^{02}
7	5.00×10^{02}
8	5.71×10^{02}
9	6.42×10^{02}
10	7.13×10^{02}

Figure 24. Maximum shear stress contours in cylinder pot and elastomer due to compression (WILREL solution).

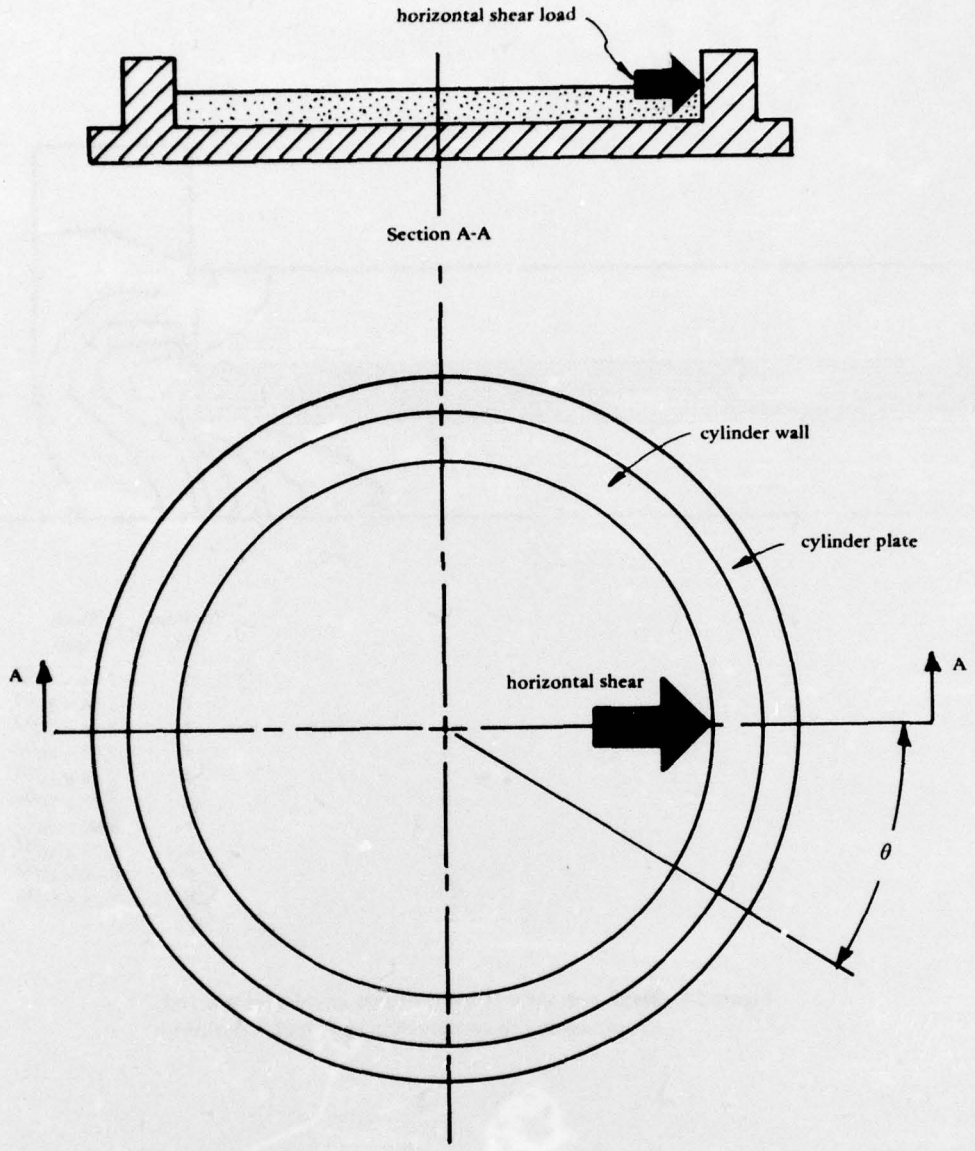

Figure 25. Plan view of idealized application of horizontal shear load for AXS finite element model.

Contour No.	Stress (psi)
1	-9.87×10^{03}
2	-7.55×10^{03}
3	-5.23×10^{03}
4	-2.91×10^{03}
5	-5.95×10^{02}
6	1.72×10^{03}
7	4.04×10^{03}
8	6.36×10^{03}
9	8.68×10^{03}
10	1.10×10^{04}

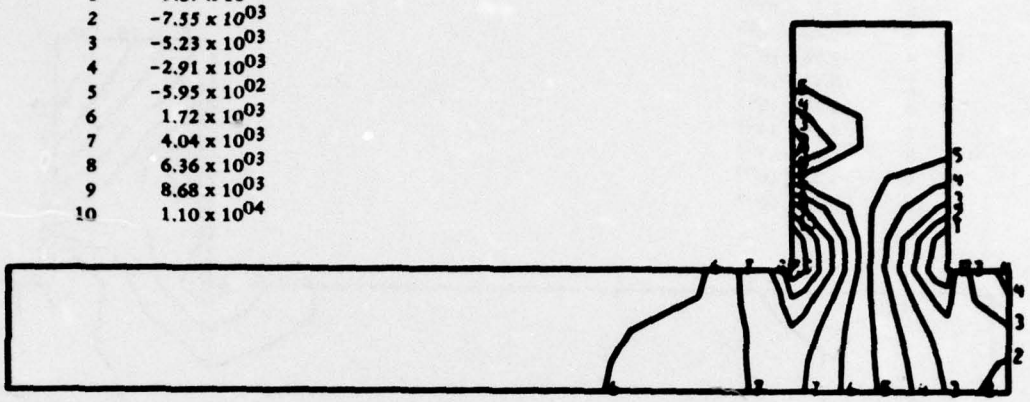

Figure 26. Vertical stress contours in cylinder pot from a horizontal shear load of 3,000 pounds (AXS solution).

Contour No.	Stress (psi)
1	-1.67×10^{04}
2	-1.41×10^{04}
3	-1.15×10^{04}
4	-8.87×10^{03}
5	-6.24×10^{03}
6	-3.62×10^{03}
7	-9.96×10^{02}
8	1.63×10^{03}
9	4.25×10^{03}
10	6.88×10^{03}

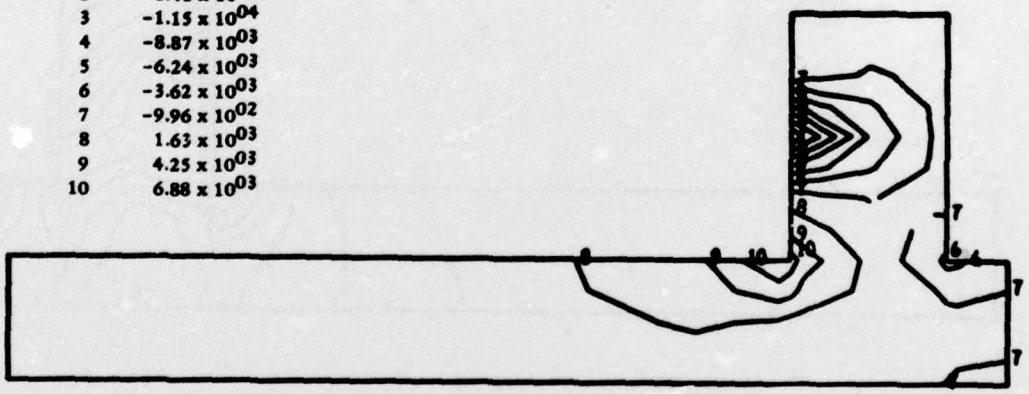

Figure 27. Radial or horizontal stress contours in cylinder pot from a horizontal shear load of 3,000 pounds (AXS solution).

Contour No.	Stress (psi)
1	-3.66×10^{03}
2	-2.53×10^{03}
3	-1.40×10^{03}
4	-2.78×10^{02}
5	8.51×10^{02}
6	1.98×10^{03}
7	3.11×10^{03}
8	4.24×10^{03}
9	5.37×10^{03}
10	6.50×10^{03}

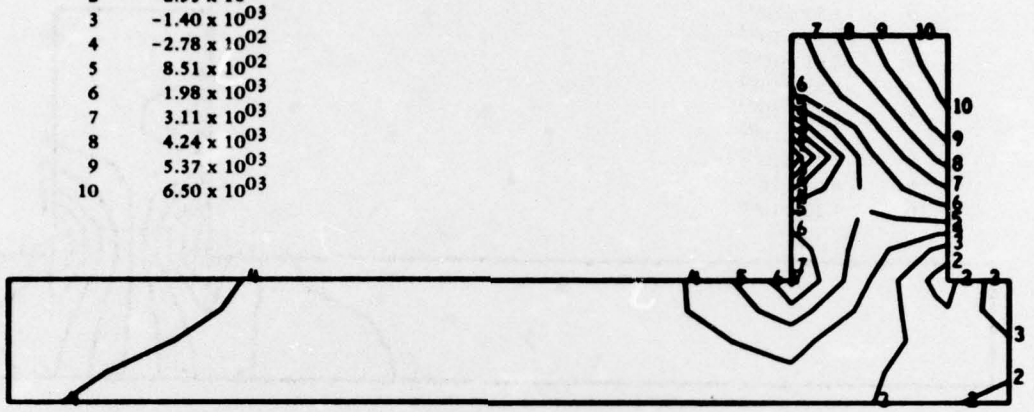

Figure 28. Tangential stress contours in cylinder pot from horizontal shear load (AXS solution).

Contour No.	Stress (psi)
1	9.86×10^{02}
2	1.94×10^{03}
3	2.89×10^{03}
4	3.84×10^{03}
5	4.79×10^{03}
6	5.75×10^{03}
7	6.70×10^{03}
8	7.65×10^{03}
9	8.61×10^{03}
10	9.56×10^{03}

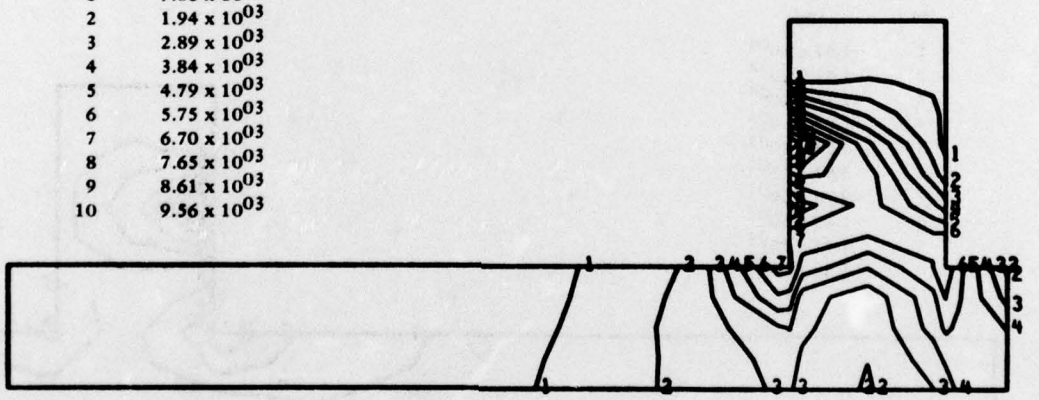

Figure 29. Maximum shear stress contours in cylinder pot from horizontal shear load (AXS solution).

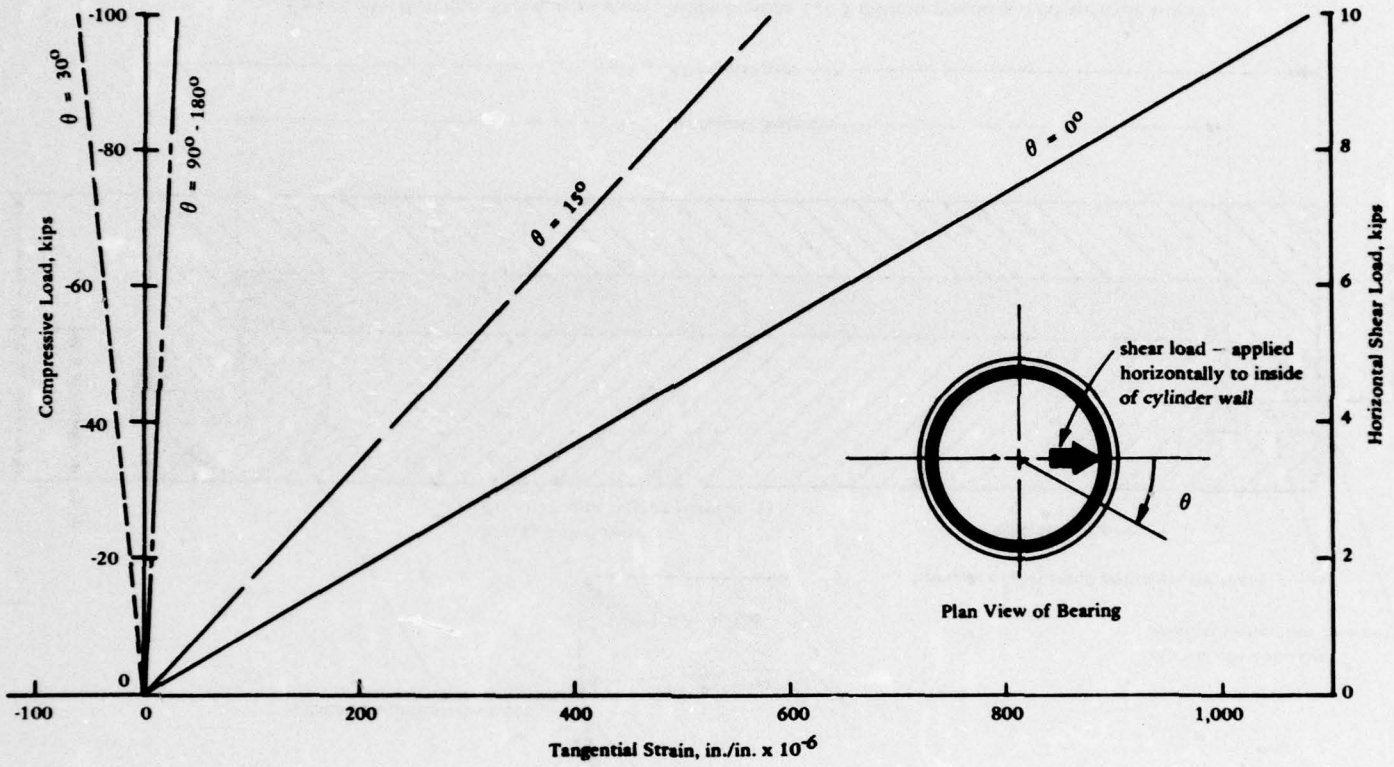

Figure 30. Tangential strain in element 12 of cylinder wall from compression load plus horizontal shear loading equal to one-tenth the compression load.

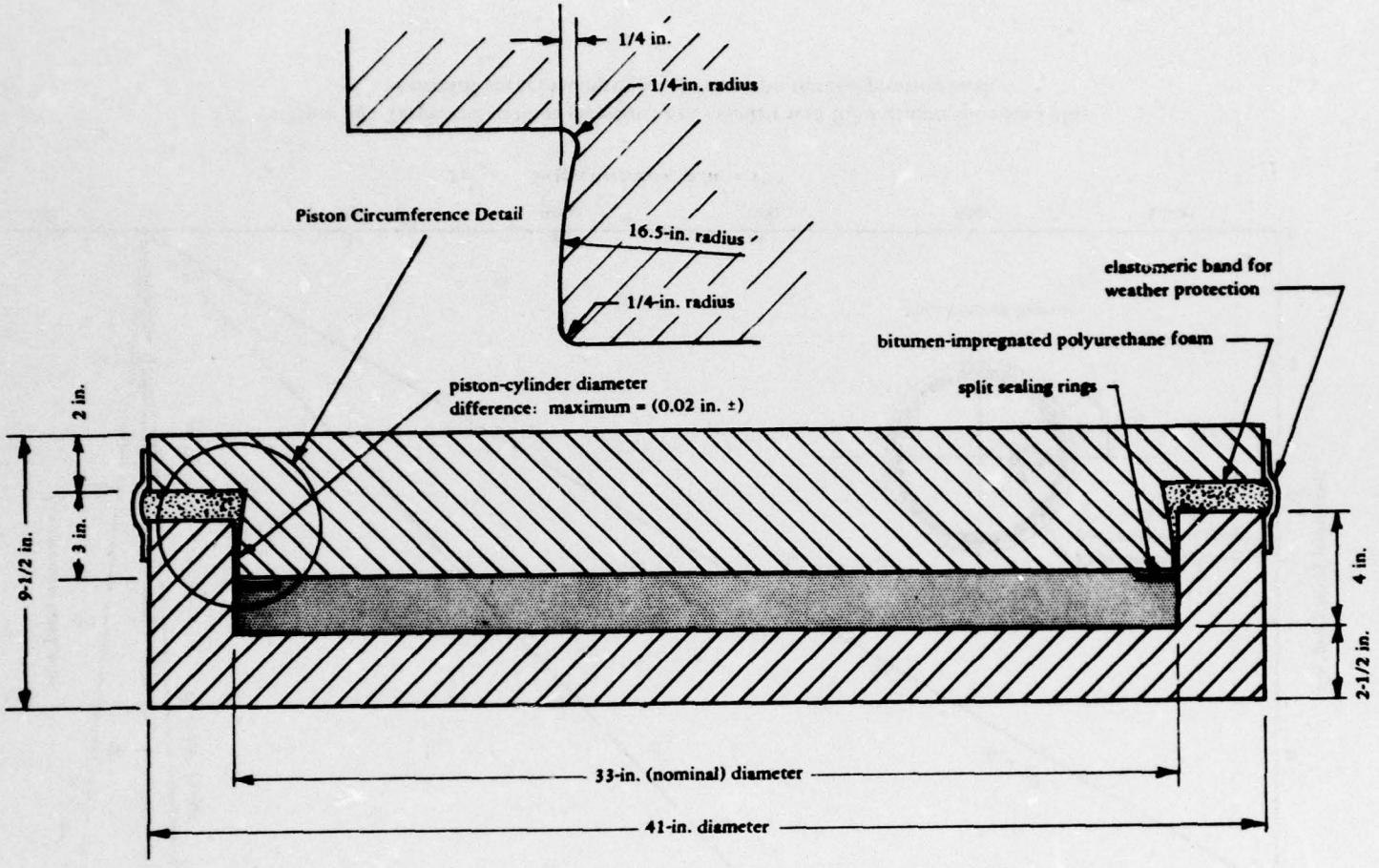

Figure 31. Recommended elastomeric hinge bearing for 3-million-pound guyed antenna tower.

DISTRIBUTION LIST

SNDL Code	No. of Activities	Total Copies	
–	1	12	Defense Documentation Center
FKAIC	1	10	Naval Facilities Engineering Command
FKN1	6	6	NAVFAC Engineering Field Divisions
FKN5	9	9	Public Works Centers
FA25	1	1	Public Works Center
–	6	6	RDT&E Liaison Officers at NAVFAC Engineering Field Divisions
–	326	328	CEL Special Distribution List No. 7 for persons and activities interested in reports on Engineering Materials